The Deformable Mirror Demonstration Mission (DeMi) On-Orbit Analysis

by

Jennifer N. Gubner

B.A. in Physics, Wellesley College (2018)

Submitted to the Department of Aeronautics and Astronautics
in partial fulfillment of the requirements for the degree of

Master of Science in Aeronautics and Astronautics

at the

MASSACHUSETTS INSTITUTE OF TECHNOLOGY

June 2021

Author .....
Department of Aeronautics and Astronautics
May 18, 2021

Certified by .....
Kerri L. Cahoy
Associate Professor, Aeronautics and Astronautics
Thesis Supervisor

Accepted by .....
Zoltan Spakovsky
Professor, Aeronautics and Astronautics
Chair, Graduate Program Committee

THIS PAGE INTENTIONALLY LEFT BLANK

The Deformable Mirror Demonstration Mission (DeMi) On-Orbit Analysis

by

Jennifer N. Gubner

Submitted to the Department of Aeronautics and Astronautics
on May 18, 2021, in partial fulfillment of the
requirements for the degree of
Master of Science in Aeronautics and Astronautics

Abstract

The Deformable Mirror Demonstration Mission (DeMi) is a 6U CubeSat mission to demonstrate the use of a 140 actuator microelectromechanical system (MEMS) deformable mirror (DM) and a closed-loop adaptive optics (AO) system in space. DeMi launched to the International Space Station (ISS) on the NG-13 Cygnus resupply mission on February 15, 2020 and was deployed from the ISS into a 51° inclination, 423 km average altitude low-Earth orbit on July 13, 2020. The expected mission lifetime of DeMi was 6 months, however DeMi continues to be operational 9 months post deployment. During its lifetime, DeMi has completed several internal observations with the DM and both imagers using the internal laser source. The team is now working toward external observations of stars and demonstrations of closed-loop wavefront control. The biggest driver of mission success is spacecraft and component health. Looking at spacecraft data over time helps to characterize spacecraft performance and inform adjustments to the lifetime estimate. Additionally, telemetry analysis can alert the operations team of anomalies and provide useful information for resolving those anomalies. This thesis analyzes the spacecraft telemetry received between July 13, 2020 and April 4, 2021 and discusses trends and anomalies in the data. This work provides an overview of spacecraft and payload on-orbit health to date and provides recommendations on paths forward for anomaly resolution.

Thesis Supervisor: Kerri L. Cahoy
Title: Associate Professor, Aeronautics and Astronautics

THIS PAGE INTENTIONALLY LEFT BLANK

Acknowledgments

I would like to extend a very special thank you to my advisor, Professor Kerri Cahoy, who has given me incredible guidance and support throughout my graduate education and my undergraduate involvement with STAR Lab. Thank you for helping me grown as a student and a person and allowing me to take on responsibilities within the DeMi project.

I would also like to thank the DeMi team for their support, advice, and encouragement. I would specifically like to thank Rachel Morgan, Joey Murphy, Bobby Holden, Christian Haughwout, Paula do Vale Pereira, Greg Allan, and Ewan Douglas. Without the help and support of each of you, this work would be impossible. Thank you for making my experience on the team so enjoyable and educating. Thank you to John Merk and Danilo Roascio for your management of the project.

Thank you to my friends and family, especially Sydney, for putting up with my weird hours for operating the spacecraft and for listening to me talk about the project to almost no end.

I would also like to thank Blue Canyon Technologies for their support and guidance on the spacecraft bus systems. I would specifically like to thank Steve Stem and Bryan Button for answering my many questions and helping me understand the spacecraft.

The DeMi project is sponsored by DARPA and has been managed by Aurora Flight Sciences, a Boeing Company.

THIS PAGE INTENTIONALLY LEFT BLANK

Contents

List of Figures

List of Tables

THIS PAGE INTENTIONALLY LEFT BLANK

Chapter 1

Introduction

This thesis is a continuation of the project originally developed by Dr. Anne Marinan in her 2016 Ph.D. thesis [13] and is an extension of the author's undergraduate thesis [9]. It builds upon the prior work presented with the exciting addition of on-orbit performance analysis[1].

1.1 Project Motivation

1.1.1 Exoplanet Direct Imaging

Since it was first proposed in 1953 by H.W. Babcock, adaptive optics (AO) has been increasingly used on ground-based telescopes to correct for the effects of atmospheric turbulence on observations [4]. With the miniaturization of AO components, these capabilities can be applied to space-based experiments such as exoplanet direct imaging. While imaging astrophysical objects in space is usually not affected by atmospheric turbulence, other AO correctable factors can still affect the resolution and contrast of the image. These factors include dynamic noise generated by the reaction wheels of the spacecraft, thermal variations within the spacecraft due to changes in solar illumination throughout its orbit, and optical misalignment or imperfections inherent to the system or induced by launch or deployment [2].

[1]Sections 1.1 and 1.2 of this chapter contain similar content to the author's undergraduate thesis, [9], as this thesis is a continuation of the same project.

AO correctional capabilities in space are particularly useful in several main applications [12]. One use of AO is to improve coupling of signals to fiber for ground-to-satellite and satellite-to-satellite laser communication, enabling higher data rate communication signals. AO can be applied to high-contrast imaging of dim celestial objects. The DeMi mission can be categorized in the celestial object imaging category, as it is intended to demonstrate capabilities for direct imaging of Earth-like exoplanets. Specifically, AO can be the critical difference in reaching the necessary contrast ratio to image Earth-like exoplanets that are typically 10^{10} times fainter than their host star [20][22].

The correctional capabilities of AO systems can also enable the use of larger and less expensive optics on space telescopes because optical imperfections can be actively corrected. The use of AO can improve imaging performance and stretch the limits of what scientists can observe.

1.1.2 Adaptive Optics Systems

DeMi's AO system has three main components: a deformable mirror, a wavefront sensor, and a camera. The component at the center of the mission and the center of the AO system is the deformable mirror (DM). The job of the DM is to supply physical corrections to the path length of the incoming wavefront. There are different types of DMs with different sizes, actuation methods, and configurations. Some examples of these are discussed in [11] for ground-based systems. The DM on DeMi is a microelectromechanical systems (MEMS) DM. MEMS DMs are convenient for use in space because of their compact size, low weight and power, low actuator mass, and high actuator density [2]. The wavefront sensor (WFS) captures and records the incoming wavefront, as shown in Figure 1-1. The goal of the WFS is to provide an estimate of the shape and a measurement of the deviations in the wavefront. There are different types of wavefront sensors, including curvature sensors, pyramid sensors, and Shack-Hartmann wavefront sensors [23]. DeMi has a Shack-Hartmann WFS (SHWFS), which uses an array of microlenslets and a CMOS imager to capture its measurements. Once the wavefront is captured by the WFS, a closed-loop con-

trols system reconstructs the incoming wavefront, measures the wavefront errors, and supplies a correction shape to the DM. When the DM receives the correctional shape from the WFS algorithm, it actuates the various sections of the mirror to reshape itself into the corrected shape. This correctional cycle repeats itself to continually make adjustments to the wavefront as the light enters the system. Finally, the image plane sensor captures a point spread function (PSF) of the reference source that incorporates the changes made by the DM and the wavefront sensing algorithm. Figure 1-1 shows a schematic of a typical AO system. See Section 1.1.3 for more information on the specific DeMi configuration.

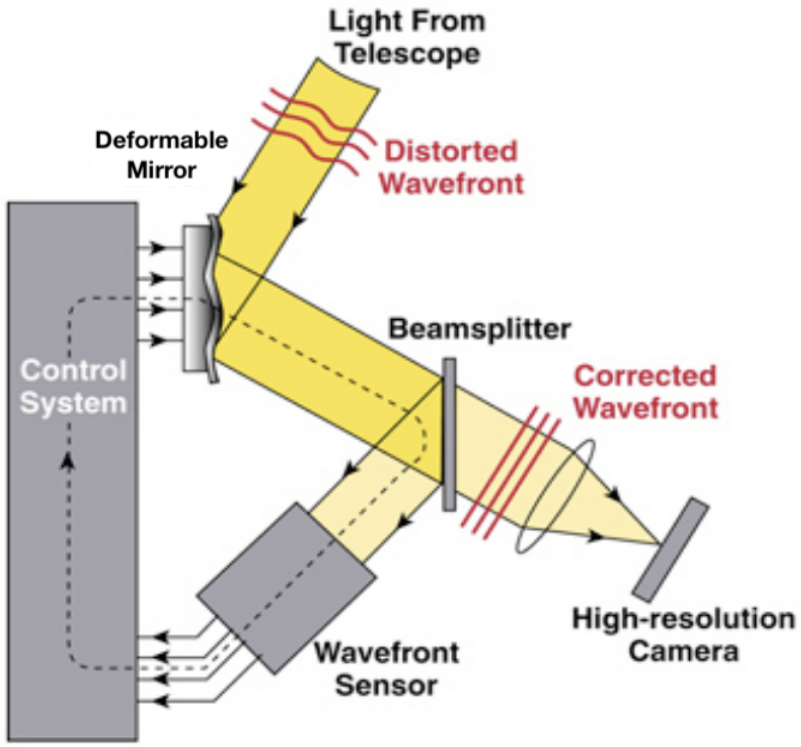

Figure 1-1: A generic representation of an AO system. A perturbed wavefront enters the optical system and is reflected through the system by a DM. A portion of the light (amount determined by the beamsplitter) is transmitted to an image sensor and the rest of the light is reflected to the WFS. The WFS records the incoming wavefront and a closed-loop algorithm supplies a corrective shape to the DM. The corrected wavefront is recorded by the high resolution camera [15].

1.1.3 Mission Objectives and Requirements

Prior to the DeMi mission, high actuator count MEMS DMs, which are a key component to a space-based AO system, were not qualified or characterized for use in space. The objective of DeMi, a 6U (30 cm × 20 cm × 10 cm) CubeSat mission, is to demonstrate the use of AO in space, as well as to characterize, and increase the technology readiness level (TRL) of a 140-actuator MEMS DM. References [2], [9], and [17] have more details on the specific science requirements of the mission.

The components on the DeMi payload and the mission's science requirements informed the spacecraft environmental, power, and pointing requirements. In order to operate the payload components, the payload optical bench must remain between 0 °C and 30 °C. In order to minimize thermal-induced misalignments of the optical system, the payload should maintain a temperature of 20 ± 4°C during operations [1] . Throughout the entirety of the mission, the payload must remain within the survival temperature range of −20 °C to 70 °C. In addition to maintaining the temperatures of the spacecraft, the bus must provide power to the payload on a 5 V line and two separate 3.3 V lines. The spacecraft battery voltage should not be below 11.5 V. The pointing stability of the spacecraft should be less than $10''$ in all three axes [14].

1.2 Mission Overview

1.2.1 Introduction to CubeSats

CubeSats were first introduced in 1999 and are a type of small satellite, whose standard was developed by the California Polytechnic State University (Cal Poly), designed to improve access to space by reducing the cost and development time required for space missions [6]. The specification for CubeSats provides the size of each satellite based on the number of units, or U's of volume. Each U is a 10 cm × 10 cm × 10 cm cube. The DeMi CubeSat is a 6U and is configured in a 30 cm × 20 cm × 10 cm shape with about 4.5U of space dedicated to the scientific payload and the other 1.5U dedicated to the spacecraft bus electronics and attitude determination and control

systems (ADCS). With the growing popularity of CubeSats, the methods of deployment of these satellites have also become increasingly standardized. Some of the DeMi mission requirements are therefore derived from the CubeSat design and deployment standards.

1.2.2 DeMi Configuration

The DeMi spacecraft can be broken out into two main parts: the spacecraft bus and the payload. The spacecraft bus was provided by Blue Canyon Technologies (BCT) and is a 6U XACT bus. The payload, designed and built by the team at MIT is contained in approximately 4.5U of the 6U bus.

The bus provides all of the critical support for the mission. In order to maintain the appropriate temperatures, the bus is equipped with several temperature sensors to record thermal variations throughout the spacecraft and two sets of two kapton heaters. One set is mounted on the interface between the bus and the payload, and the other set is mounted on the underside of the payload optical bench. The specific configuration of heaters is discussed in more detail in Section 4.2. The main spacecraft battery can be charged up to 12.3 V by the two solar panels. To provide communication between the satellite and the spacecraft operators, the spacecraft uses one of two UHF radios. A Cadet radio is used for high data rate communication with the NASA Wallops Flight Facility ground station, and a Lithium radio is used for communication with the MIT ground station. See Chapter 2 for more details on the communication configuration. The bus is also responsible for the attitude determination and control (ADCS) of the spacecraft. To provide the necessary pointing accuracy, the bus uses 3 reaction wheels, a star tracker, three packages of 4 sun sensor diodes, an inertial measurement unit (IMU), a GPS system, torque rods, and a magnetometer. Section 4.5 discusses the on-orbit performance of these ADCS components.

The DeMi payload includes an optical bench with all of the mounted optical components, a baffle to block out stray light at the external aperture, a payload electronics stack, and two camera boards. Figure 1-2, taken from [18], shows the fully integrated payload and bus system with the baffle in the top left, the payload

electronics stack to the right of the baffle, the payload optical bench on the bottom and the camera boards mounted to the right of the optical bench.

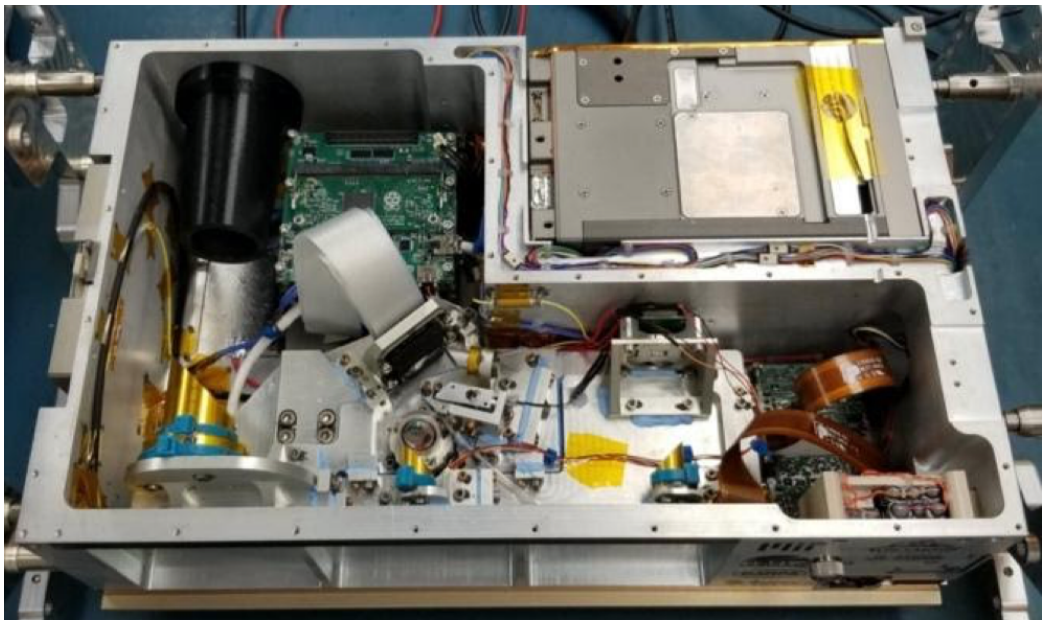

Figure 1-2: Image of the fully integrated spacecraft. The bus is the main box that houses all of the components and the bus electronics are in the top right corner, taking up about 1.5U of the spacecraft. The payload is housed in the remaining L-shaped volume. The spacecraft baffle, in black, is mounted to the top left of the internal volume. Next to the baffle is the payload electronics stack in green. The electronics stack includes the two Raspberry Pi compute modules and the DM driver boards. The payload optical bench is mounted in the lower part of the bus volume and the two camera boards are mounted to the right of the payload optical bench. This image is taken from [18].

The optical bench consists of a series of off-axis parabolic mirrors (OAPs), field mirrors, two complementary metal-oxide semiconductor (CMOS) cameras, a Shack-Hartmann Wavefront Sensor (SHWFS) and a Boston Micromachines Corporation (BMC) 140-actuator MEMS DM. The optical layout is shown in Figure 1-3. The payload directs the light source, either internal or external, through a beamsplitter and uses part of the beam for the closed-loop wavefront correction and the other part to image the point spread function (PSF). All of the components and operations are controlled by two Raspberry Pi Compute Module 3 flight computers. References [1], [9], and [19] discuss the optical design in more detail.

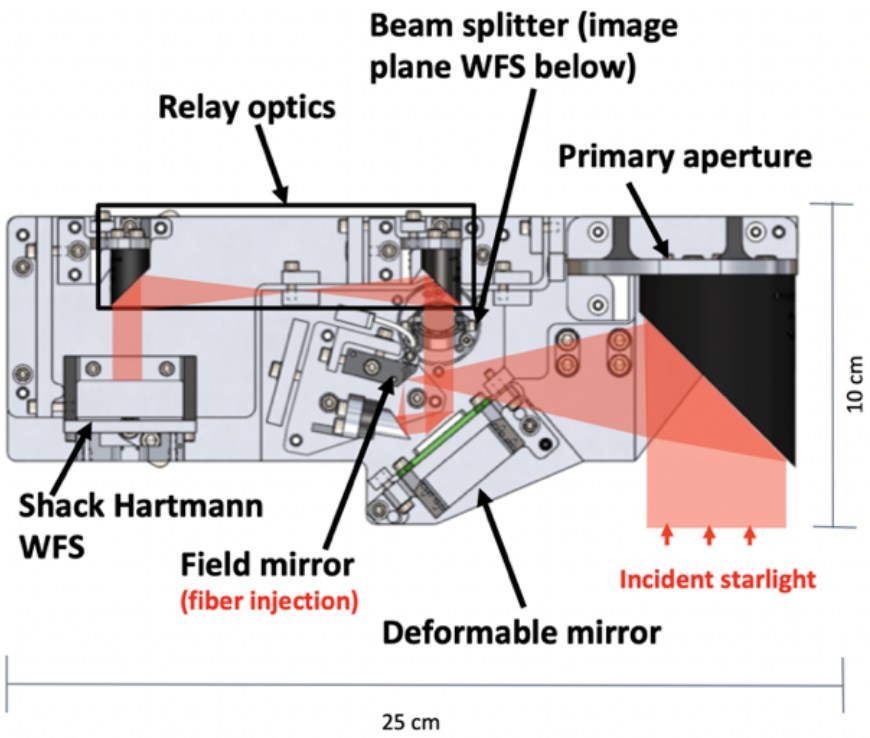

Figure 1-3: Optical path of the DeMi payload, taken from Morgan, et al. [19].

1.2.3 Concept of Operations (ConOps)

DeMi is configured to be able to perform both internal and external observations during its lifetime. The internal observations are used to characterize the DM and to test the closed-loop wavefront control system with a 635 nm internal laser. The external observations are intended to demonstrate the use of the AO system on astronomical targets. Before each science operation, the operations team checks the battery voltage levels and the payload temperatures, in addition to the spacecraft pointing, if doing an external observation. After the checks, the operators send a command to the satellite to perform an operation either immediately or for execution at a later time. At the specified time, the spacecraft powers on the required components for the specific mode of operation. If commanded to do so, the payload will take baseline measurements and image frames to measure dark current and sensor bias measurements prior to capturing an image of the target. Figure 1-4 shows a diagram of the mission concept of operations and Figure 1-5 shows a block diagram of the various

modes of operations.

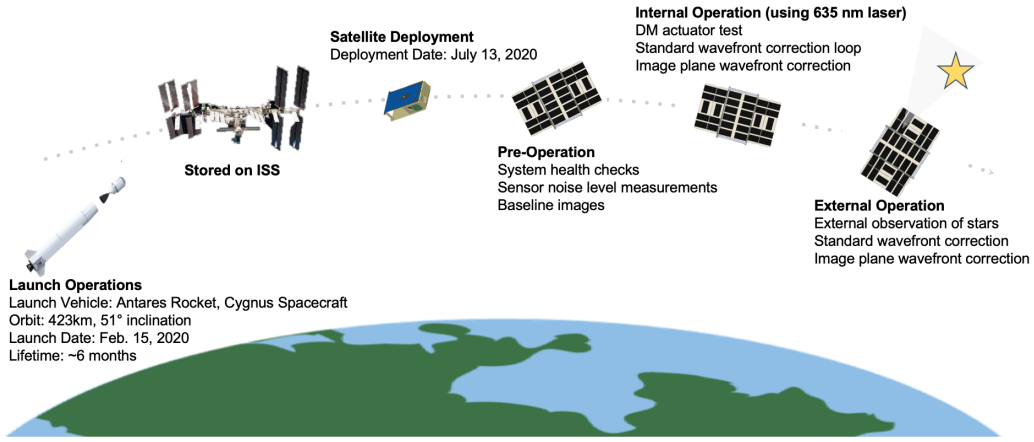

Figure 1-4: Graphic of the concept of operations for the DeMi mission. DeMi aboard the NG-13 ISS resupply mission inside a Cygnus spacecraft on February 15, 2020. DeMi was stored aboard the ISS until July 13, 2020 when it was deployed into a 51° inclination orbit at a mean altitude of 423 km above the Earth. After deployment, solar array actuation, and detumble, the spacecraft was commissioned for regular operations. These operations include pre-operation, or calibration, internal operation using an internal laser as the target of interest, and external operation using an astronomical target.

1.2.4 Orbit and Lifetime Estimates

Prior to launch, the DeMi mission had an estimated lifetime of about 6 months. The lifetime estimate comes from a combination of component lifetime estimates, radiation tolerances, thermal cycling lifetimes, and orbital decay historical data for CubeSats. DeMi was deployed into a circular orbit from the ISS with an initial mean altitude of 423 km and an inclination of 51°. As of April 22, 2021, DeMi is at a mean altitude of 403 km, having dropped 20 km in 9 months. Figure 1-6, created by graduate student Joey Murphy, shows a comparison between the ASTERIA CubeSat mission and DeMi. Both missions have similar form-factors and thus, it is expected that DeMi will follow an orbital decay rate similar to the ASTERIA mission. Based on the historical data from the orbital decay of ASTERIA, it is expected that DeMi has about 700 days left before it de-orbits. However, it is possible that some of the critical science components will not last as long.

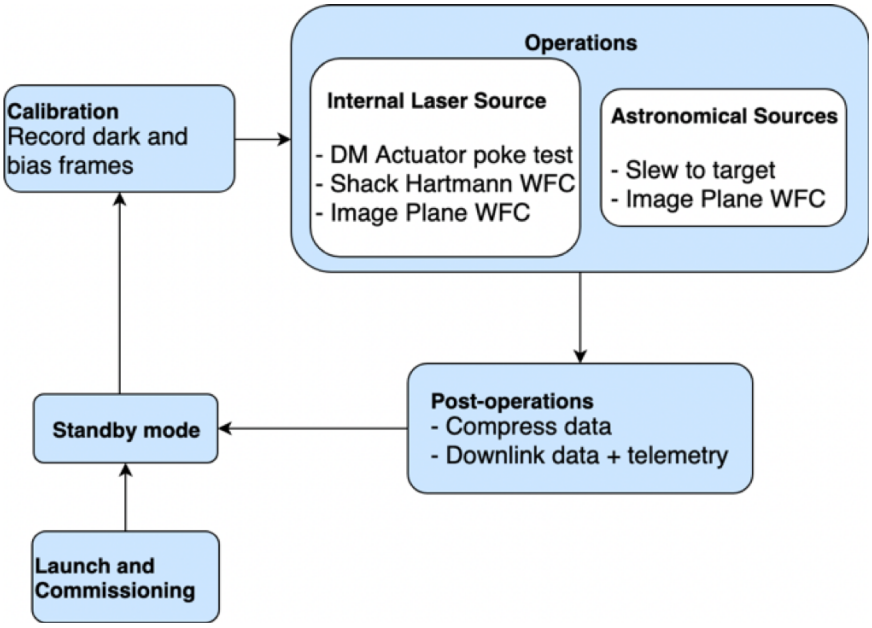

Figure 1-5: Block diagram of the different modes of operation available on the DeMi mission. After launch and commissioning, the satellite progressed into standby mode waiting for the operation commands. From there, the operations team can command the satellite to take calibration images, followed by either internal or external mode. Both modes have several experiment options that are executed depending on what the team is trying to observe. Finally, the data is compressed and downlinked via one of the radios on the bus. Diagram taken from [18].

1.3 Thesis Contributions

This thesis analyzes the DeMi spacecraft on-orbit data between deployment on July 13, 2020 and April 4, 2021 for both the payload and the spacecraft bus. Chapter 2 provides an overview of the command and data handling system that enables the retrieval of the data from the spacecraft. Chapter 3 looks at the payload performance including sensor status and completed operations to-date. Chapter 4 discusses the performance of the spacecraft bus including thermal management, power distribution, and attitude determination and control. Finally, Chapter 5 summarizes the findings from the spacecraft data and outlines the future work for the DeMi mission.

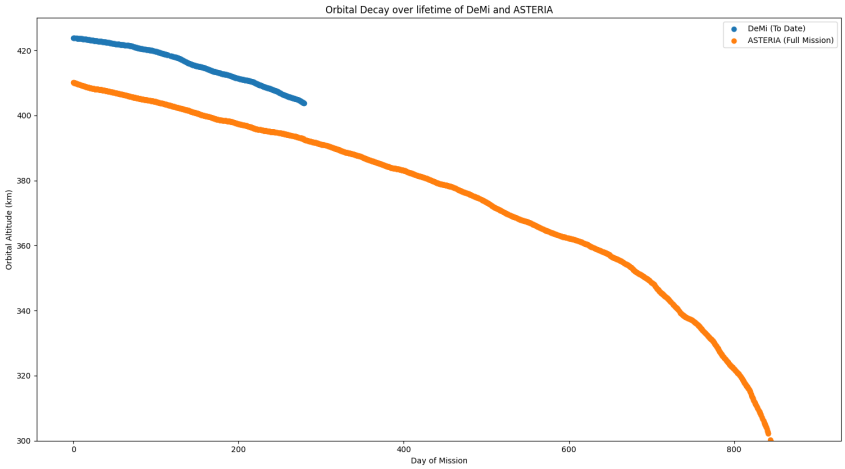

Figure 1-6: Plot created by graduate student Joey Murphy showing the orbital decay of the DeMi mission through April 22, 2021 along with the orbital decay of a previous CubeSat mission, ASTERIA, with a similar form-factor. After 283 days in orbit, DeMi has decayed by about 20 km and it is estimated that approximately 700 days remain before DeMi de-orbits.

Chapter 2

Command and Data Handling Configuration

Command and data handling infrastructure is one of the most important subsystems for any space mission. Without it, there would be no way to command operations or return data to the ground. Command and data handling (C&DH) is the system that manages the sending and receiving of commands and telemetry to and from the spacecraft. The DeMi mission uses two different onboard radios that interface with two different ground stations on the East Coast of the United States. Additionally, the DeMi mission uses Ball Aerospace's open-source COSMOS software [16], which provides a helpful interface to check connections with the satellite and radio, format commands to send to the satellite, format and process telemetry, execute automated scripting to send commands and check telemetry, and record entire communication sessions. Figure 2-1 shows some of the COSMOS tools that the DeMi team uses during passes with the satellite. Because the DeMi team contracted Blue Canyon Technologies (BCT) to provide the 6U bus, the team received a BCT-modified version of COSMOS upon delivery of the bus that already included the command and telemetry configurations for the bus-specific items. In addition, the COSMOS version received from BCT was configured to interface with data from both of DeMi's radios: a Lithium radio and a Cadet radio. Each radio type has a corresponding ground station setup described in more detail throughout this chapter.

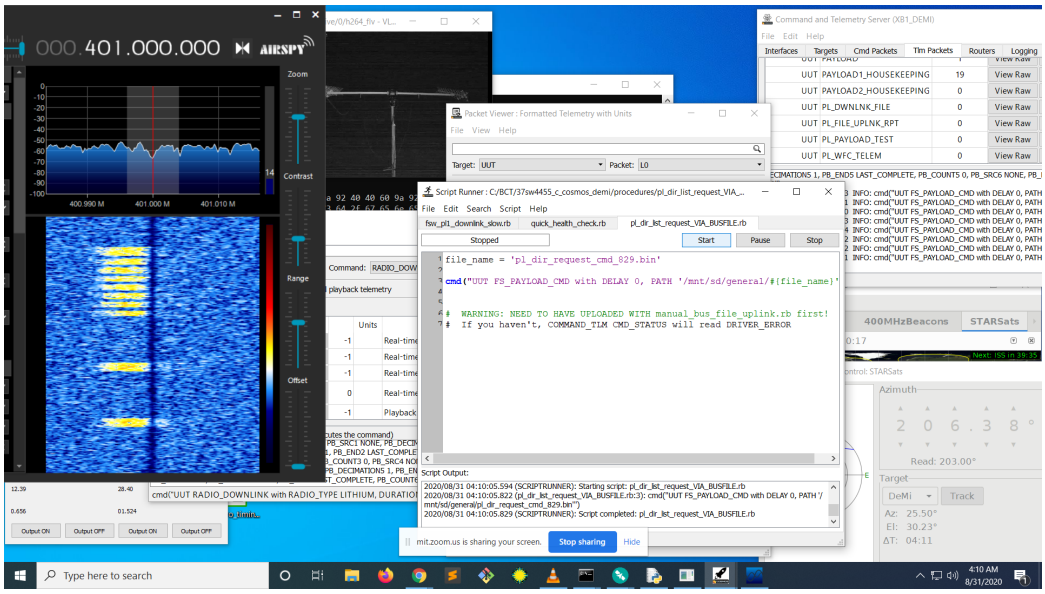

Figure 2-1: The MIT ground station configuration during a pass with DeMi. On the screen are several COSMOS tools, along with pass statistics tools and antenna control tools. The top right window, “Command and Telemetry Server,” shows the connection statistics, the “Command Sender” window (hidden behind the waterfall plot and the "Script Runner") is where the user can configure and send a command to the satellite, the window at the center, the “Script Runner,” allows the user to run scripts that automate and control the timing of commands and telemetry, and the window hidden directly behind the "Script Runner" window, “Packet Viewer,” lets the user see the various states and values in a specific telemetry packet. There are other available COSMOS tools not shown here [16].

2.1 Wallops Pipeline Configuration

The Cadet radio on the DeMi CubeSat was configured to have a direct link with the NASA Wallops Flight Facility (WFF) ground station located in Wallops Island, Virginia. This is a UHF 3 Mbps connection with a downlink frequency of 468 MHz and an uplink frequency of 449.775 MHz. The WFF ground station is connected over the network to the ground station computer located at MIT. It is from the MIT ground station computer that the team formats commands and monitors the incoming telemetry, however the WFF ground station actually sends the commands over radio frequency (RF) up to the spacecraft and receives the telemetry from the spacecraft over RF before routing it to the MIT ground station computer that is equipped with the COSMOS tool to process the telemetry. A diagram of this connection is shown in Figure 2-2.

Figure 2-2: Diagram of the connection to and from the DeMi satellite via the Cadet radio. The NASA Wallops Flight Facility has a ground station antenna that is configured to interface with DeMi's Cadet radio and route the telemetry and commands between the DeMi satellite and the MIT ground station.

The WFF ground station was intended to be the high data rate ground station used for file downlinks from the satellite. Unfortunately, the WFF ground station went off-line due to mechanical failures in September of 2020 and did not return to operations until March 22, 2021. Between July and September of 2020, when both DeMi and the WFF ground station were operational, the DeMi team was able to use the WFF ground station for over 40 overpasses to command the satellite and downlink telemetry. Since March 22, 2021, the DeMi team has successfully completed 4 WFF passes, one of which produced a mission record data volume of 3,115,984 bytes

received. Because the high data volume passes are supported by WFF, which has been offline for a majority of the DeMi mission thus far, the DeMi team has been actively working on ways to supplement the lower rate downlinks. These include modifying the MIT ground station software, working on logic to request smaller portions of files, and actively looking for other ground stations that are able and willing to support DeMi at the Cadet uplink and downlink frequencies. More information about these modifications can be found in Subsection 2.2, UHF Low-Rate Configuration.

2.2 UHF Low-Rate Configuration

The other ground station, configured in large part for a DeMi communication link by MIT graduate student Joey Murphy, is located on the roof of building 37 at MIT. This ground station is configured for UHF uplink and downlink and has been used for communications with other satellites, including MiRaTa [5]. An image of the antenna is shown in Figure 2-3. This communication link uses a Lithium radio with an uplink frequency of 449.775 MHz and a downlink frequency of 401 MHz to communicate with MIT. The Lithium has a data rate of 9600 bps and uses GMSK modulation scheme [3]. Figure 2-4 shows a diagram of the UHF low-rate configuration.

Figure 2-3: Image of the MIT ground station antenna on the roof of building 37. The MIT ground station uses a Lithium radio to communicate with the DeMi satellite with an uplink frequency of 449.775 MHz and a downlink frequency of 401 MHz.

Figure 2-4: Diagram of the connection to and from the DeMi satellite via the Lithium radio. MIT has a receive and transmit antenna located on the roof of building 37. The team formats commands and receives telemetry from the ground station computer on campus and the data is transmitted through the antenna.

Initially, the MIT ground station was intended for telemetry monitoring and operation scheduling on-board the DeMi spacecraft. Scheduling operations and receiving state of health telemetry should nominally require relatively low data rates. After the temporary decommissioning of the WFF ground station, the MIT ground station became the only working link with DeMi and was then required for file downlinks as well as the previously mentioned telemetry monitoring and operation scheduling. As discussed in Section 2.1, the file downlink process involves downlinking a large quantity of data. With only the low data rate configuration available for the DeMi mission, there were many configuration adjustments that were needed to accommodate the downlink of data.

One of the first major changes to the configuration was the way the ground station software handles the data packets. When the DeMi team switched to using the MIT ground station to receive data from the satellite, for some unknown reason the data packets coming from the Lithium radio were not reaching the COSMOS processing software, even though the Cadet radio data packets had no issue and the rest of the Lithium telemetry packets were being sent to COSMOS. The DeMi team is still looking into why this is happening for the Lithium connection and specifically the data packets only. In the meantime, Joey Murphy and the DeMi team put a lot of effort into processing the incoming data packets right as it is received through

the COM port on the ground station computer. Joey created a tool, called the COM Sniffer by the DeMi team, which intercepts the telemetry stream so that it can process the data packets before routing the data through to COSMOS. This tool is able to successfully intercept the chunks of data sent by the satellite, parse the chunks, and save them in a similar structure to that used by COSMOS.

In addition to the changes for handling data downlinks on the ground station computer, the team had to make changes to the communication architecture in order to command a file downlink from the Lithium. Not only do both radios have significant differences in available data rates, but they also have different maximum command and telemetry packet lengths. This difference in command packet length led to problems when requesting a file for downlink because that specific command exceeded the maximum command length on the Lithium. As a result, MIT graduate student Bobby Holden and the DeMi team created a work-around in which the team uploads several shell scripts to the payload that move the file and execute the downlink when it is run. While this fix works and is the best option we have at this moment for Lithium-specific data downlinks, it is a multi-step process that usually requires several passes to upload and execute and is very inefficient as compared with the single downlink request command.

The temporary loss of the WFF ground station also brought about other inefficiencies in the DeMi team's ability to receive data. One of the major inefficiencies arose out of the inability to easily downlink directory listings from the satellite, as these are treated the same as a file downlink and would require the multi-step shell script uplink process described above. Because the DeMi team was not able to easily view the existing file list for downlinks, and the command to downlink a file requires knowing the exact name and location of the file, the DeMi team implemented a re-naming strategy to re-name the top 9 desired files with generic names that are easier to request without errors.

2.3 Ground Station Statistics

As of April 5, 2021, the DeMi mission has completed 534 successful passes, where success means that data has been received from the satellite. Due to the unavailability of the WFF ground station for a large portion of the mission so far, the majority of DeMi's passes have been taken by the MIT ground station. Figure 2-5 shows a breakdown of the number of successful passes taken by each ground station. As of April 5, 2021, the campus ground station at MIT is nearing 500 DeMi passes and the WFF ground station is nearing 50.

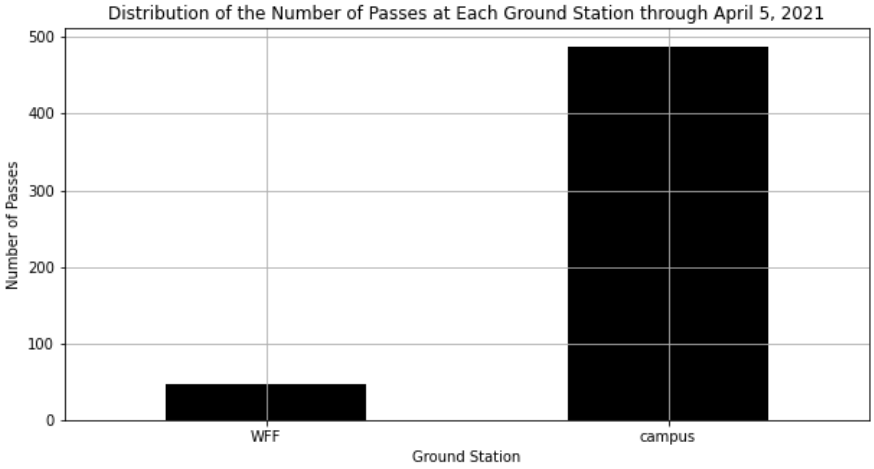

Figure 2-5: Distribution of the number of passes by ground station. The WFF ground station is the NASA Wallops Flight Facility ground station and the campus ground station is the MIT ground station located on the roof of building 37. This data is from the start of the mission in July, 2020 to April 5, 2021.

Throughout the mission, the campus ground station has collected on average about 31 kB of data from the satellite each pass with a maximum of 125.748 kB from a single pass. The WFF ground station has collected 402 kB of data on average each pass, and holds the record for the most data volume collected on a single DeMi pass at 3115.984 kB. A distribution of data volume received per pass by ground station is shown in Figure 2-6.

Chapter 3 discusses how some of this data is used to understand payload health behavior over the mission lifetime.

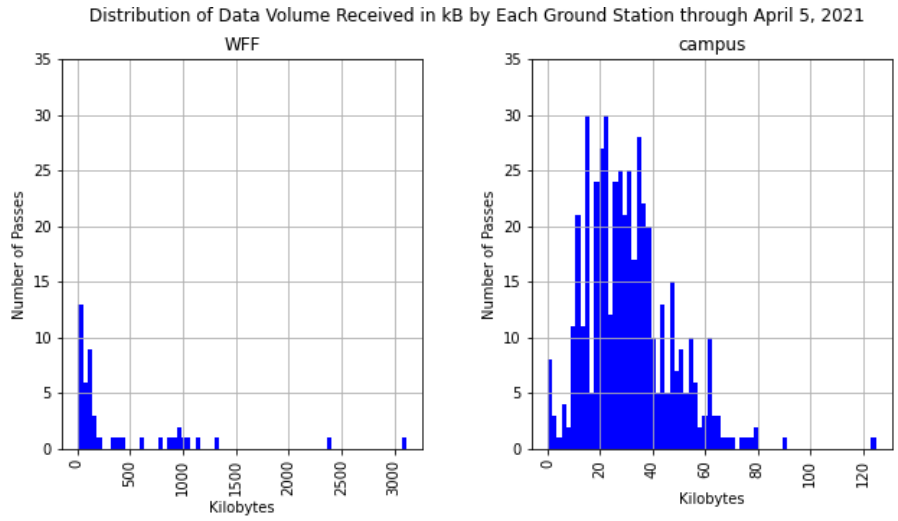

Figure 2-6: Distribution of data volume, in *Kilobytes*, received per pass by ground station through April 5, 2021.

Chapter 3

Payload Operations Analysis

The DeMi payload consists of the payload optical bench, a baffle for external observations, an electronics stack, and two camera boards. The optical bench configuration, which was described in Chapter 1, holds all of the optical components including both imagers and the deformable mirror (DM). The electronics stack consists of two main flight computers, referred to as Payload 1 and Payload 2, and several DM driver boards. The electronics stack is discussed in more detail in Section 3.2. The two camera boards are connected to the electronics stack and the two imagers by cables, but they are not mounted with the electronics stack or on the optical bench.

The reader should keep in mind that the data presented here is only the data received from the satellite, and is therefore limited in quantity. Due to the ground station configuration and pass priorities, the operators have not downnlinked all of the payload playback telemetry data. Therefore, the data presented here may not completely represent the payload behavior on-orbit. However, the data provides insight into the status of the payload health. The data is plotted with times shown in UTC.

3.1 Deformable Mirror and Driver Status

The main science component of interest for the DeMi mission is the DM. The DM is the basis for the wavefront control demonstration and for the technology demonstra-

tion. Without the DM, the mission's science objectives are unattainable. Because DM operation is so critical to mission success, the driver boards that control the DM actuation are also critical. The driver boards were designed in-house by MIT graduate student Christian Haughwout, whose master's thesis covers the details of design and implementation [10].

Once the satellite was deployed and commissioned, the team began checking out all of the on-board systems. One of the first tests the operations team attempted was a poke test. The poke test is a diagnostic test used during ground and environmental testing, and the team has a solid understanding of the baseline poke test performance. A poke test is an operation where each DM piston is actuated to a specified percentage of the maximum displacement, and the actual displacement of each piston is measured by the Shack-Hartmann wavefront sensor (SHWFS) and the payload flight electronics. By running the poke test, the team can confirm that the internal laser, the SHWFS, the DM, and the payload flight electronics are working as expected. Additionally, this test produces a smaller data file because the displacement measurements are returned rather than an actual image, making this test a good choice for on-orbit testing of component functionality and for measuring DM performance.

On August 4, 2020, shortly after the beginning of the mission, the team successfully captured and downlinked a poke test that confirmed DM actuation, laser operation, and SHWFS operation. In data analysis done by MIT graduate student Rachel Morgan, deflection of the mirror in space was compared with ground testing, and the results from in space agreed with ground data with a median $\frac{|ground-space|}{ground}$ of 5.35%. On September 11, 2020, the team captured an image with the image plane camera that confirmed the laser was still working and that the image plane camera was functional.

Shortly after these images were taken and downlinked, the Wallops Flight Facility went offline and remained offline for a significant portion of the mission to-date. The DeMi operations team continued attempting to collect data, but downlinking the new data was a very slow process and resulted in a lot of inconclusive results due to lack of data. On March 25, 2021, the team was able to confirm that the laser and SHWFS

were still operational, however data from December, 2020 and March, 2021 that the team received only recently, showed no signs of DM actuation.

Currently, the team's top priority is figuring out why the DM actuation is not working as expected and how it can be resolved. The team is actively working on ruling out issues with:

- The laser
- The imagers
- The DM
- The DM driver boards
- The power delivery to the DM
- Command delivery to the DM
- The Raspberry Pi flight computers
- The Raspberry Pi interface with the DM driver boards

So far, imager and laser operation has been confirmed through the capturing of spot-field images on the SHWFS and PSFs on the image plane camera. It is possible that the issue could be with the DM. The DM could be sensitive to the space environment which, over time, may have caused damage to the component. If this is the only issue, the team may not be able to conclusively confirm it, but it will become increasingly likely as the other possible issues are ruled out. Currently, the team is working on confirming DM driver board operation as well as power and command delivery to the DM. The original intention was to include a complete capture of this data in the payload housekeeping telemetry. However, due to time constraints, not all DM telemetry measurements were implemented before delivery, but several implementations are planned for future uplink. Several scripts to record power delivery to the DM are in development and will soon be uplinked to the satellite. Once the team is

able to return the contents of the logs created by these scripts, the power delivery and DM commanding can be confirmed or addressed.

Another system that could be contributing to DM actuation failure is the Raspberry Pi flight computers. Through analysis of on-chip temperature measurements, discussed in more detail in Section 3.2, it appears that the temperatures of the Raspberry Pis have been consistently above a widely recognized limit where the CPU begins to throttle its processing rates. It is possible that the flight computers are not behaving as expected, and the DM is not receiving properly formatted commands. To rule this out as an issue, the team will be performing a series of thermal tests on the ground and will be looking more closely at the flight computer temperatures during operations from the environmental testing campaign. Future testing will also be done on the Raspberry Pi interface with the DM and driver boards if the power analysis and flight computer temperature analysis come back inconclusive.

3.2 Flight Computer Status

The two flight computers for the DeMi payload are Raspberry Pi Compute Module 3's. They were selected for their small size, configurability, and flight heritage. Figure 3-1 shows the DeMi electronics stack. The top two boards are the Raspberry Pis and the bottom boards are DM driver boards. The top Raspberry Pi board is referred to as Payload 2 and the bottom Raspberry Pi is referred to as Payload 1. Each of the two flight computers are equipped with two SD cards, A and B. The primary flight computer configuration we have been using is Payload 1 on SD card A. Payload 1 is in charge of capturing images on the Shack-Hartmann wavefront sensor (SHWFS) and Payload 2 is responsible for capturing images on the image plane sensor. Both Payload 1 and Payload 2 can control the DM and perform closed-loop wavefront control, however the two flight computers cannot operate at the same time.

Throughout most of the mission, the DeMi team has been using the Payload 1 flight computer to try to capture images on the SHWFS. Section 3.4 discusses these operations in more detail. Two telemetry items of particular interest are the payload

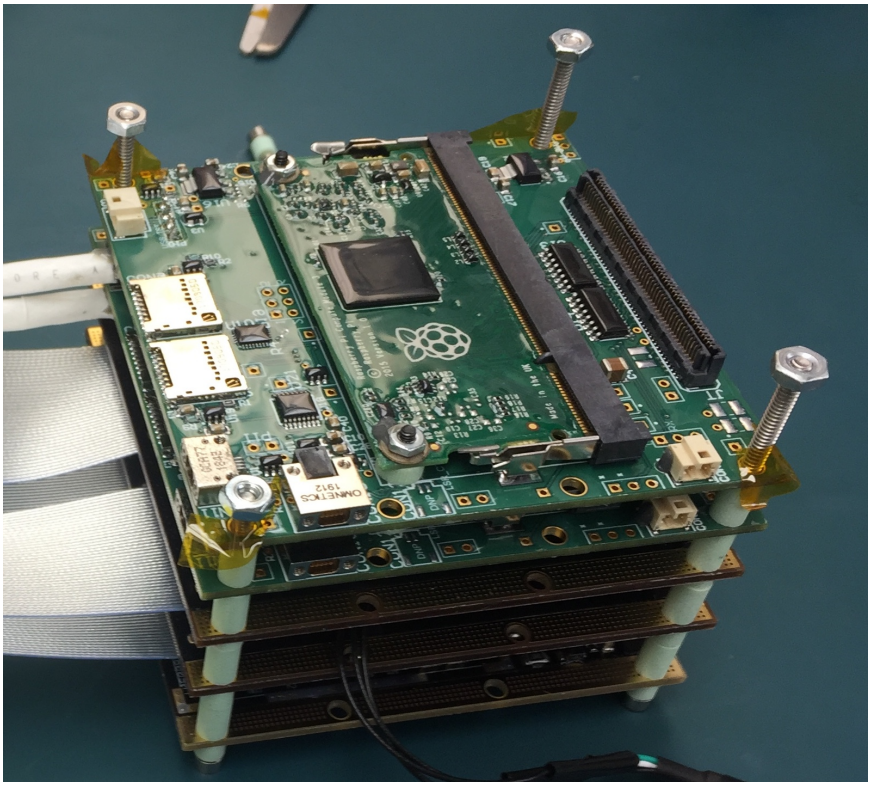

Figure 3-1: Figure of the DeMi electronics stack. The top two boards are the Raspberry Pi flight computers and the bottom three boards are the DM driver boards.

flight computer Raspberry Pi temperatures. Each Raspberry Pi is equipped with an on-chip silicon temperature sensor that measures the temperature of each flight computer. These temperatures are included in the payload housekeeping telemetry packets, which are returned to the operations team when the flight computers are powered on. During payload operations, the Raspberry Pi temperatures should not be above the CPU throttling temperature of 80 °C, where the on-board clock frequency is throttled down to minimize thermal loading. Figure 3-2 shows the Payload 1 flight computer temperature over time with the throttling limit shown as the gold horizontal line and the commanded Payload 1 operation times shown as the vertical blue dashed lines. Figure 3-3 shows the same, but for Payload 2. During most of the payload operations, except for the successful DM actuation on August 4, 2020, the Raspberry Pi temperatures appear to be at or over the throttling limit. On August 4, 2020, the temperatures appear to be cooler and closer to 70 °C. Throttling may be contributing to some of the DM issues discussed in Section 3.1. To rule out flight computer throttling as a contributing factor to the DM performance issue, the on-orbit Raspberry Pi temperatures will be compared with the Raspberry Pi temperatures taken during ground performance and environmental testing. Additionally, the team will work to better monitor Raspberry Pi temperatures prior to commanding science operations to mitigate taking images when the temperatures are close to the known throttling limit.

3.3 Imagers and Laser Status

While the DM has not shown recent evidence of actuation, the team has confirmed that the SHWFS, the image plane sensor, and the laser are still functional.

Although complete DM power telemetry is not yet available in the payload housekeeping telemetry, temperature data from both imager sensors and housings is available. Figure 3-4 and 3-5 show temperatures from the SHWFS and image plane sensor respectively. The orange points represent sensor temperatures and the blue points represent body temperatures. In most cases, sensor and body temperatures agree

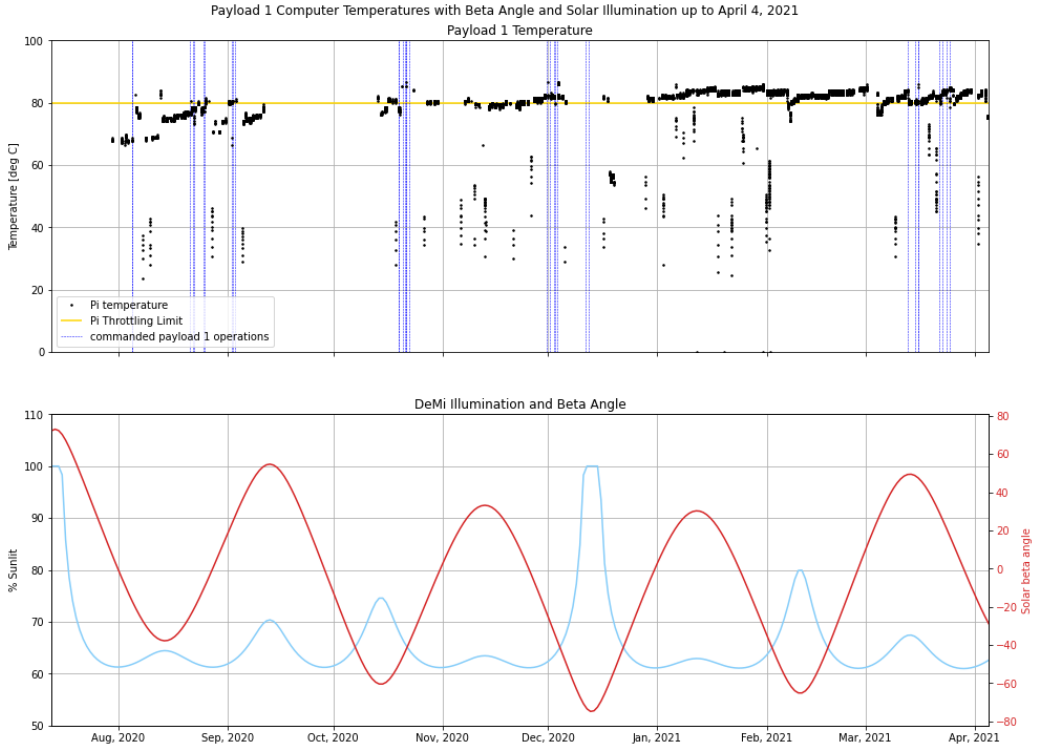

Figure 3-2: The top subplot shows Payload 1 Raspberry Pi temperature plotted as the black points with the throttling limit shown as the gold horizontal line and commanded Payload 1 operations shown as blue vertical dotted lines. The operations line at the beginning of August demonstrated successful commanding of the DM. The bottom subplot shows the beta angle (red) in degrees and the percentage of an orbit that DeMi is illuminated by the sun (light blue).

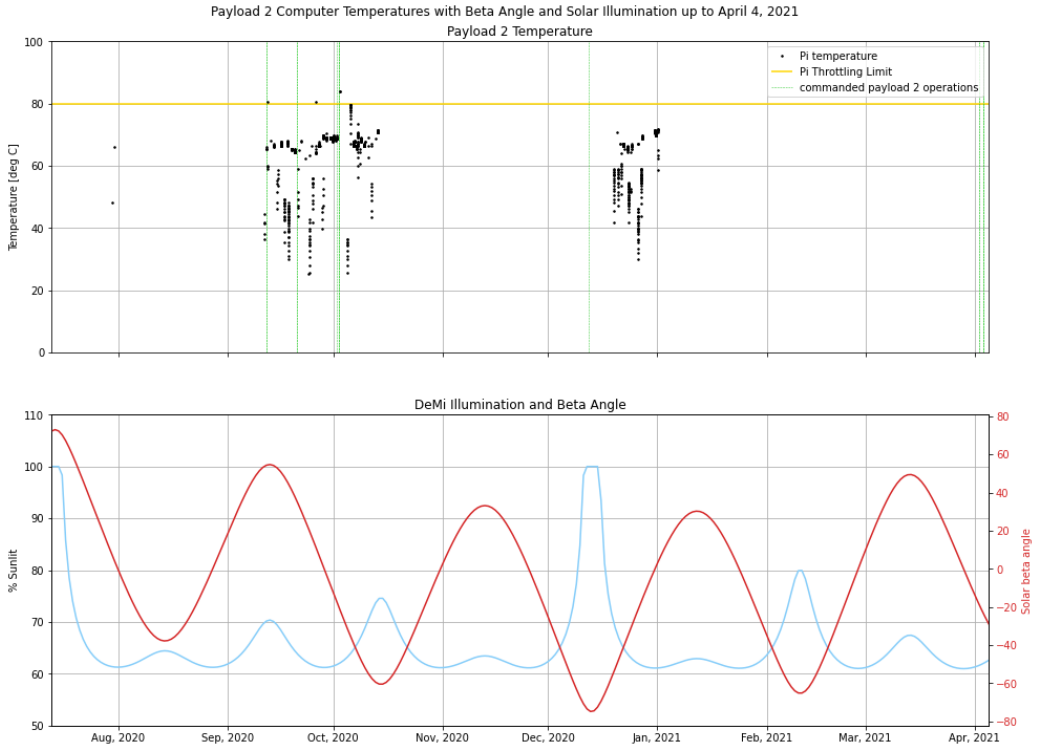

Figure 3-3: The top subplot shows Payload 2 Raspberry Pi temperature plotted as the black points with the throttling limit shown as the gold horizontal line and commanded Payload 2 operations shown as green vertical dotted lines. The bottom subplot shows the beta angle (red) in degrees and the percentage of an orbit that DeMi is illuminated by the sun (light blue).

to within 5 °C. The values on the -1 °C line are when the payload was on, but the wavefront controller and cameras had not been turned on yet. The values on the 0 °C line are from when the cameras were turned on but had not been used yet to take an image. The temperatures from all of the commanded operations appear to be between 20 °C and 35 °C for the SHWFS and between 15 °C and 30 °C for the image plane. The operating range for the cameras we are using on DeMi is between 0 °C and 50 °C [21], so the cameras have been within the operating limits during all operations.

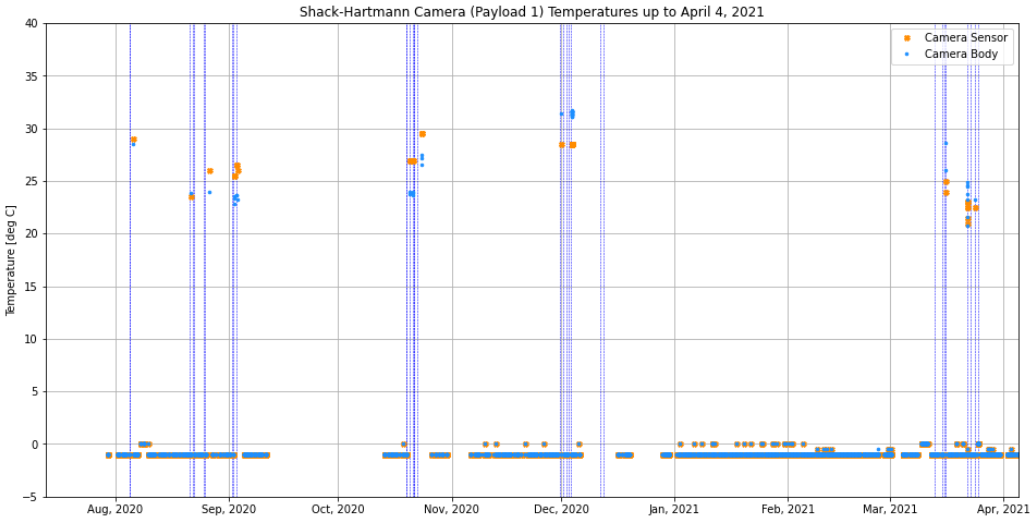

Figure 3-4: Shack-Hartmann wavefront sensor temperatures with commanded Payload 1 operations shown as the blue dotted vertical lines. The imager sensor temperature is shown as the orange points, and the imager body temperature is shown as the blue points.

3.4 Payload Operations Progress

Overall, the operations team has commanded and successfully generated data files for almost 45 science operations as of April, 2021. These commanded operations include poke tests, images on the SHWFS, images on the image plane sensor, and calibration images which include bias and dark frames. Tables 3.1 and 3.2 show all of the successfully captured images and data files. Not all of the images and data collected have yielded successful results, but the images and data were successfully captured by the payload.

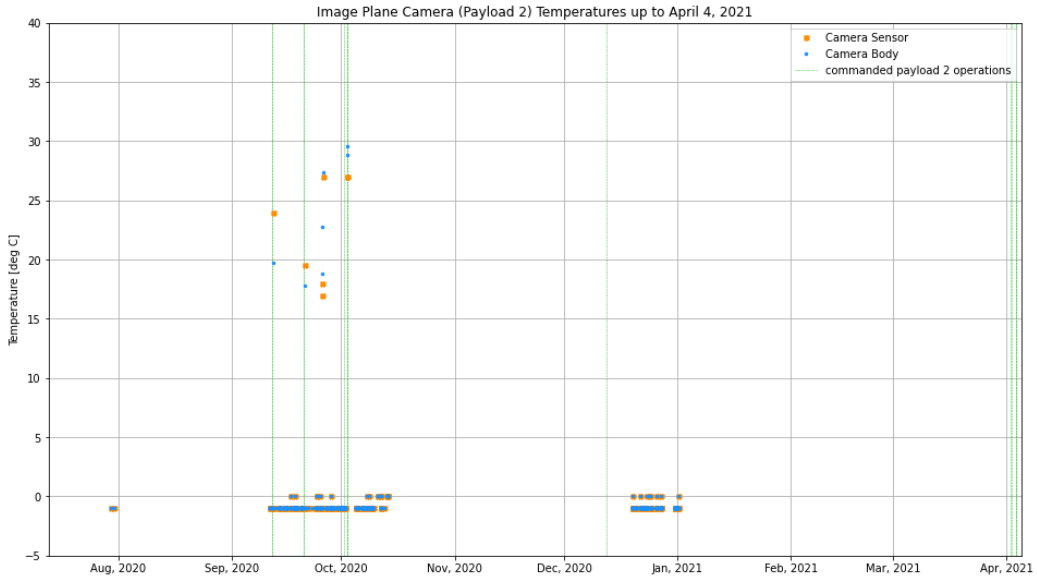

Figure 3-5: Image plane camera temperatures with commanded Payload 2 operations shown as the green dotted vertical lines. The imager sensor temperature is shown as the orange points, and the imager body temperature is shown as the blue points.

The successful DM actuation data from August 4th was a commanded poke test to 30% actuation. Additionally, the team has downlinked images from the SHWFS which showed that the sensor and laser are working, but that the DM actuation is not.

3.5 Overall Payload Health Discussion

Overall, the payload remains semi-operational. The payload computers are both responding to commands from the operations team, the cameras are functional, the laser is working, and telemetry is successfully being transmitted to the ground stations. Unfortunately, the team has been unable to confirm DM actuation since the WFF ground station returned to operations.

As discussed in [9] and [18], the main objectives for the DeMi mission are to:

1. Demonstrate on-orbit performance of a 140 actuator Boston Micromachines Corporation DM,

2. Raise the technology readiness level (TRL) of the microelectromechanical sys-

tems (MEMS) DM to a 7,

3. Correct static and dynamic wavefront errors to less than 100 nm RMS, and

4. Measure low order aberrations to $\frac{\lambda}{50}$ precision and $\frac{\lambda}{10}$ accuracy.

DeMi has met objectives 1 and 2, but has yet to complete 3 and 4. Having measured DM actuator displacement on orbit successfully, the team hopes to continue with demonstrating wavefront correction. The DM actuation is a critical component of the wavefront correction demonstration, and that is why all of the team's efforts are focused on getting the DM operational again. When, or if, the DM becomes operational again, the team will demonstrate wavefront correction with the internal laser before moving to demonstration on external targets. A future plan for the DeMi mission is also to try to capture an image of the moon or other astrophysical target on the image plane camera, although this operation would not be related to any of the mission objectives that take top priority.

For the payload to be successful, the spacecraft bus needs to be healthy and operating as expected. Chapter 4 analyzes spacecraft health and performance throughout the mission and discusses how certain payload operations may contribute to or be affected by spacecraft operations.

Payload 1 Operations	
Date of Operation (UTC)	Type of Operation
8/4/20 19:55	poke test (30%)
8/21/20 07:29	dark, bias
8/22/20 06:39	spotfield, dark, bias
8/22/20 13:19	poke test (15%)
8/25/20 06:08	poke test (30%)
8/25/20 12:30	poke test (30%)
9/2/20 02:34	dark, bias
9/2/20 09:01	spotfield
9/3/20 01:52	poke test (15%)
10/19/20 15:24	poke test (30%)
10/19/20 15:37	spotfield
10/20/20 14:36	poke test (15%)
10/21/20 09:06	poke test (15%)
10/21/20 13:42	poke test (30%)
10/21/20 14:01	bias, dark
10/22/20 12:58	poke test (15%)
11/30/20 14:53	poke test (30%)
12/1/20 14:04	poke test (30%)
12/2/20 13:26	poke test (30%)
12/2/20 19:23	poke test (30%)
12/2/20 21:12	poke test (30%)
12/3/20 14:00	poke test (30%)
12/11/20 14:22	poke test (30%)
12/12/20 15:01	poke test (30%)
3/13/21 04:02	wfc
3/15/21 04:54	zernike
3/15/21 22:02	poke test (90%)
3/16/21 02:49	spotfield
3/22/21 00:39	spotfield
3/22/21 20:35	spotfield
3/24/21 00:29	spotfield
3/25/21 01:02	spotfield

Table 3.1: Table of Payload 1 operations captured between July 13, 2020 and April 4, 2021. Operations include poke tests to varying percentages of actuation, calibration dark and bias frames, spotfield images of the laser on the detector of the SHWFS, and DM commands like wfs and zernikes that apply shapes to the DM.

Payload 2 Operations	
Date of Operation (UTC)	Type of Operation
9/11/20 23:08	psf
9/20/20 19:04	zernike
9/20/20 19:06	zernike
10/1/20 21:22	zernike
10/2/20 14:00	zernike
10/2/20 14:01	poke actuator (30%)
10/2/20 14:02	poke actuator (30%)
12/12/20 15:04	psf
4/2/21 05:04	poke actuator (30%)
4/2/21 06:40	poke actuator (30%)
4/3/21 12:19	zernike
4/3/21 12:20	zernike
4/3/21 12:22	zernike

Table 3.2: Table of Payload 2 operations captured between July 13, 2020 and April 4, 2021. Operations include individual actuator pokes to varying percentages of actuation, point spread function (PSF) images of the laser on the detector of the image plane camera, and DM zernike commands that apply shapes to the DM.

THIS PAGE INTENTIONALLY LEFT BLANK

Chapter 4

Bus Operations Analysis

As discussed in Chapter 1, the DeMi payload is integrated into a Blue Canyon Technologies (BCT) 6U XACT bus. The BCT bus provides the DeMi mission with all of the necessary communication, power, thermal, attitude determination and control, and command and data handling subsystem interfaces. Because the BCT bus acts as the life support system for the satellite, it is critical that all of the bus components function as required throughout the mission lifetime. This chapter looks at all of the critical spacecraft bus components and analyzes the bus performance throughout the mission to-date.

The reader should keep in mind that the data presented here is only the data received from the satellite, and is therefore limited in quantity. Due to the ground station configuration and pass priorities, the operators have not downnlinked all of the spacecraft health data. Therefore, the data presented here may not completely represent the spacecraft behavior on-orbit. However, the data provides insight into the status of the payload health. The data is plotted with times shown in UTC.

4.1 Storage

One of the main purposes of the bus flight electronics is to receive data from the DeMi payload, format the data into telemetry packets, and downlink the data as requested by the operations team on the appropriate radio. Additionally, the bus flight

electronics store important health related data in order to downlink the spacecraft health status to the operations team upon request. The spacecraft data is split up into 5 partitions: payload, flight software (FSW), state of health (SOH), tables, and line. Payload is all of the data received from the payload. This includes images and payload housekeeping data that the payload sends to the bus to transmit back to Earth. The FSW partition holds information about the current flight software and its configuration. SOH contains information on the state of health of the spacecraft and its operation. Line data is used for the star tracker buffer, and tables are stored information about the data configuration on the satellite. Figure 4-1 shows the usage of all of the partitions on the SD cards together on one plot. In addition to each individual partition, the spacecraft reports on the total usage.

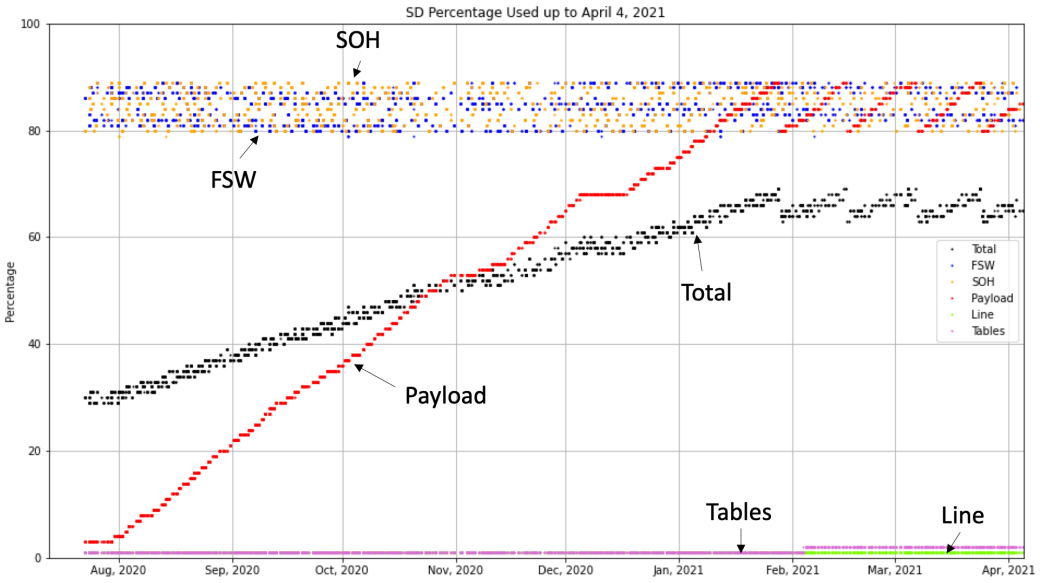

Figure 4-1: All of the spacecraft data partitions SD card usage shown as a percentage over time. Black is the total usage, red is the payload usage, blue is the FSW usage, orange is the SOH usage, green is the line usage, and purple is the table usage.

To maintain storage capabilities on the SD cards, when the payload data reaches 90% usage, the flight software will delete the oldest payload data until the payload usage returns to 80%. From the second subplot in Figure 4-2, you can see that at the end of January, the payload usage reached the limit and the flight software performed the expected clean-up of the data. Currently, the DeMi team is considering manually

clearing out some of the payload data in order to preserve the more important files and images. Below the payload partition, the FSW and SOH usages look sporadic and seem to remain in between 80% and 90% usage. There is likely no discernable trend with this data because it is constantly being stored on the SD cards and only a small portion of the data has been received by the ground station. If we were to receive all of the spacecraft data, we would likely see a quick increase and clear out of the SOH and FSW partitions in a similar pattern as the payload partition. FSW and SOH usage data also indicates that those partitions are being cleared out appropriately once they reach 90%. The total usage reflects all of the clearing of payload, FSW, and SOH data and appears to remain under 70% usage. Overall, the SD card management appears to be performing as expected.

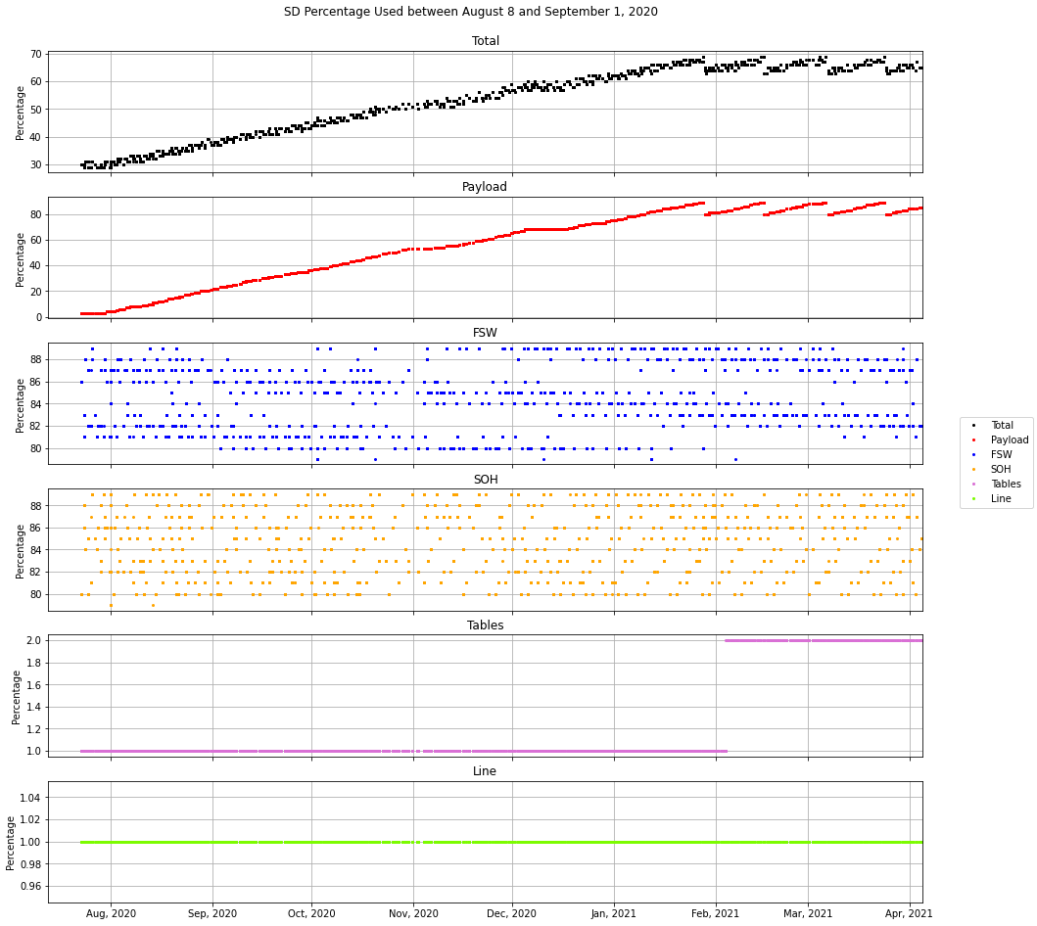

Figure 4-2: SD percent usage of the 5 spacecraft data partitions along with total usage shown in separate subplots with different y-axis scales to show details. The colors represent the same data values as in Figure 4-1.

4.2 Temperatures

As stated in Chapter 1, thermal management of the spacecraft is critical for the safe operation of the payload. The acceptable temperature ranges are defined by the payload and bus operational and survival limits. The acceptable temperature range for payload operation is between 0 °C and 30 °C, with an ideal temperature of 20 ± 4°C. However, the payload can survive, with all components off, between -10°C and 65 °C. These ranges are limited by the most thermally sensitive component on the payload structure. The DM has the lowest maximum operating temperature of 30 °C and the cameras have the highest minimum operating temperature of 0 °C. Additionally, the bus operational temperature range is from -20°C to 60 °C.

The bus is responsible for measuring the spacecraft temperatures at various points on the structure and turning on or off the spacecraft heaters when appropriate. One of the most important temperature sensors on the spacecraft is located on the payload optical bench. Figure 4-3 shows the placement of this temperature sensor on the payload. This sensor ensures that the optical bench, and most importantly the deformable mirror (DM), remains within the required temperature limits at all times. Additionally, when the temperature reading reaches threshold values, the heaters are triggered on or off. Figure 4-4 shows the heater placements on the underside of the payload optical bench. During spacecraft survival mode, where none of the payload components are on, the heater-on setpoint is 10 °C and the heater-off setpoint is 15 °C. During payload operational mode, where the payload components are on and potentially capturing images, the heater-on set point is at 15 °C and the heater-off setpoint is at 20 °C. The ideal temperature for payload operations is 20 ± 4°C.

Figure 4-5 shows the payload optical bench temperature and heater status throughout the mission. The blue points represent times when the payload heaters were in operational mode and the red points represent survival mode. The X's represent heater off points and the dots represent heater on. The operating mode heater setpoints are shown in blue at 15 °C on and 20 °C off. The survival mode heater setpoints are shown in red at 10 °C on and 15 °C off. From the available data, the payload tem-

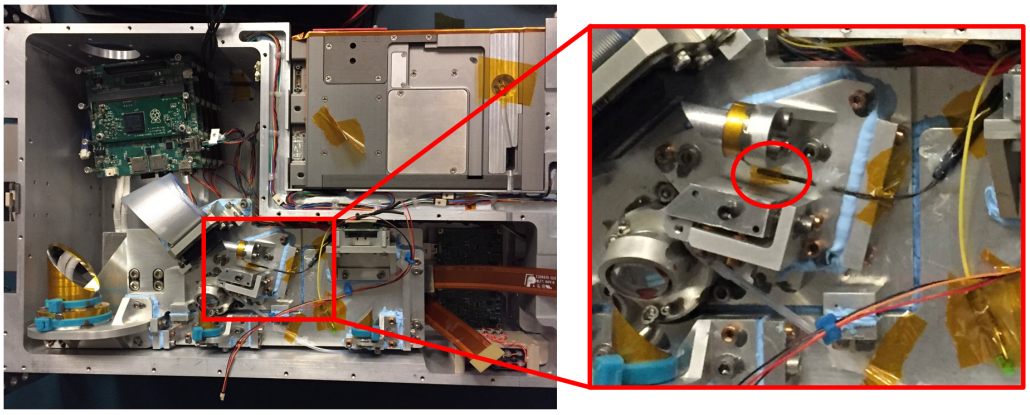

Figure 4-3: Photo showing the placement of the thermistor on the payload optical bench. (a) The red box shows the zoomed in location for the temperature sensor placement. (b) The temperature sensor is the small black wire and probe, shown inside the red circle, that is placed between the field mirror and the small off-axis parabolic mirror. This was the safest location for placing the temperature probe close to the DM, which is in the top left of the zoomed-in red box.

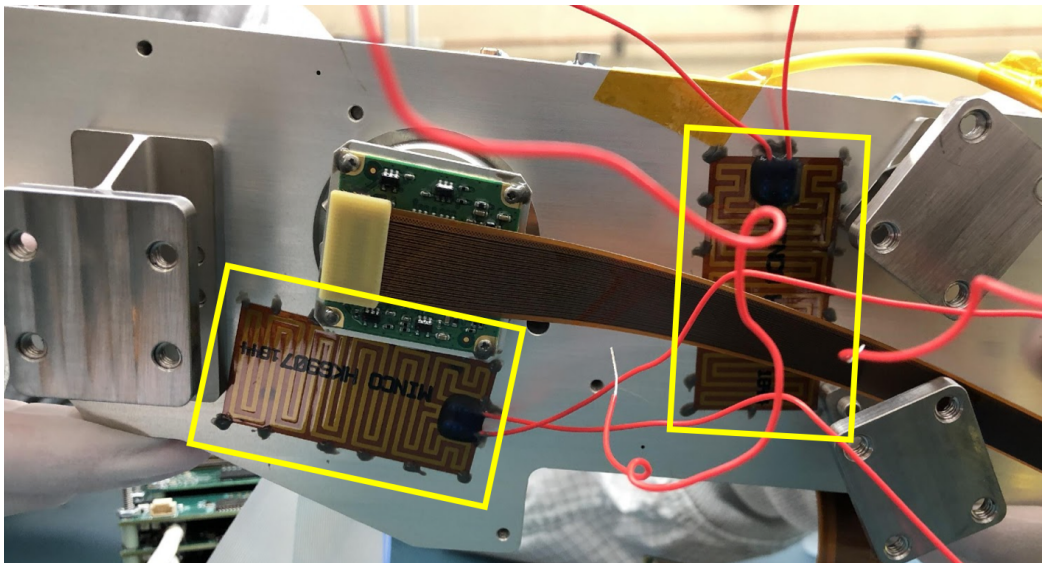

Figure 4-4: Payload heater placement on the underside of the optical bench. The two kapton heaters are shown inside the yellow rectangles. The heater in the left part of the image is placed underneath the DM and the other heater is placed close to underneath the Shack-Hartmann wavefront sensor (SHWFS). The component placements on the optical bench are shown in Figure 1-3. These heaters are automatically triggered on or off when the payload temperature sensor reaches a threshold temperature specific to the mode of operation.

perature does not drop below 10 °C at any point. Additionally, the heaters are off for a majority of the available data. Furthermore, the heaters are never on in survival mode above the survival heaters off setpoint and the same goes with the operating mode heaters. Finally, the payload optical bench temperature remains between 10 °C and 25 °C, which is within the limits of 0 °C to 30 °C required to operate the optical components. At most times, the optical bench temperature remains in the 20 ± 4°C range during operating mode.

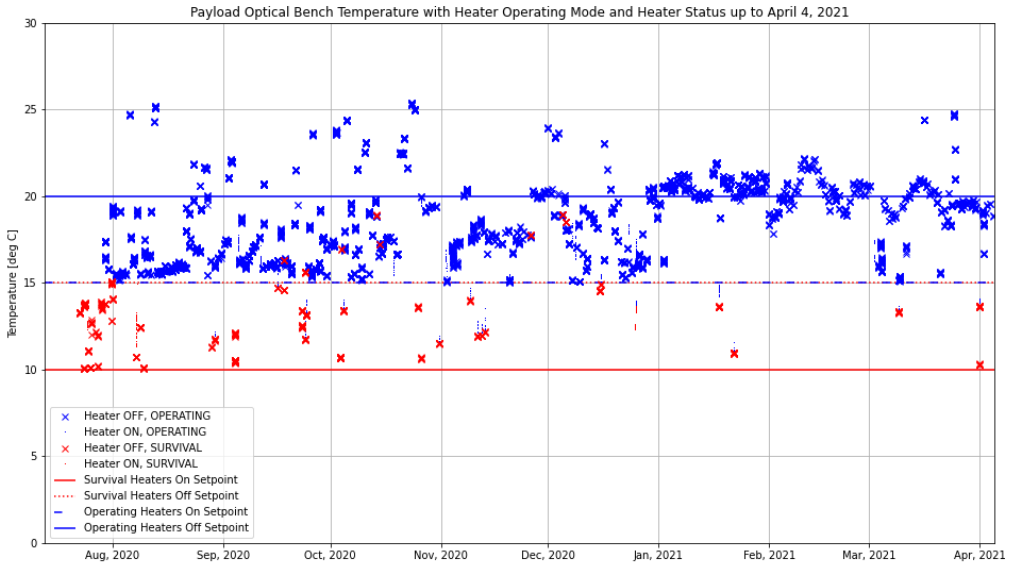

Figure 4-5: Payload optical bench temperature over the mission duration plotted with heater status and operating mode. Heater setpoints for each operating mode are also shown. The blue points represent periods of heaters in operating mode and the red points represent periods of heaters in survival mode. The X's represent heaters off and the dots represent heaters on. The operating mode heater setpoints are shown in blue with the on setpoint at 15 °C and the off setpoint at 20 °C. The survival mode heater setpoints are shown in red with the on setpoint at 10 °C and the off setpoint at 15 °C.

Figure 4-6 shows the payload optical bench temperature in the top plot and solar illumination and beta angle in the bottom plot. Solar illumination and beta angle is calculated by a script that was created by MIT graduate student Joey Murphy and is included in Appendix B. The top plot also shows vertical dotted lines that represent the times of commanded science operations for both payload flight computers. It appears that during periods of operations, the payload optical bench temperature

runs slightly higher than normal payload non-operation. On the bottom plot, solar illumination is given in terms of percent of orbit illuminated by the sun and beta angle is given in degrees. It appears that payload operations seem to have more of an impact on payload optical bench temperature than solar illumination in orbit.

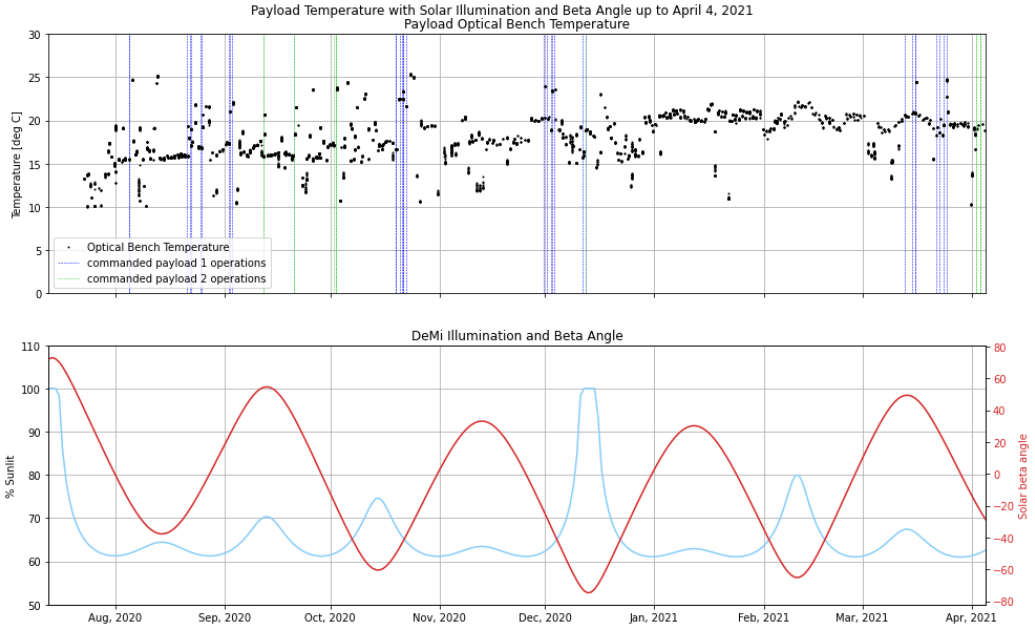

Figure 4-6: Payload optical bench temperature shown as the black points with commanded operations by both flight computers shown as the vertical lines.The bottom subplot shows the beta angle (red) in degrees and the percentage of an orbit that DeMi is illuminated by the sun (light blue).

In addition to the payload optical bench thermal management system, the bus provides thermal management for the payload/bus interface. The term interface is used here as the point of contact between the optical bench and the spacecraft bus. On the underside of the payload optical bench, three titanium standoffs attach the optical bench to the bus, as seen in Figure 4-4. These standoffs allow the payload to be significantly thermally isolated from the bus and allow some flexibility for thermal deformations [7]. The payload/bus interface is also equipped with a temperature sensor and two kapton heaters. These thermal components can be seen in Figure 4-7. The payload/bus interface heaters have the same operational and survival mode on/off setpoints as the payload heaters.

Figure 4-8 shows the payload/bus interface temperature and heater status through-

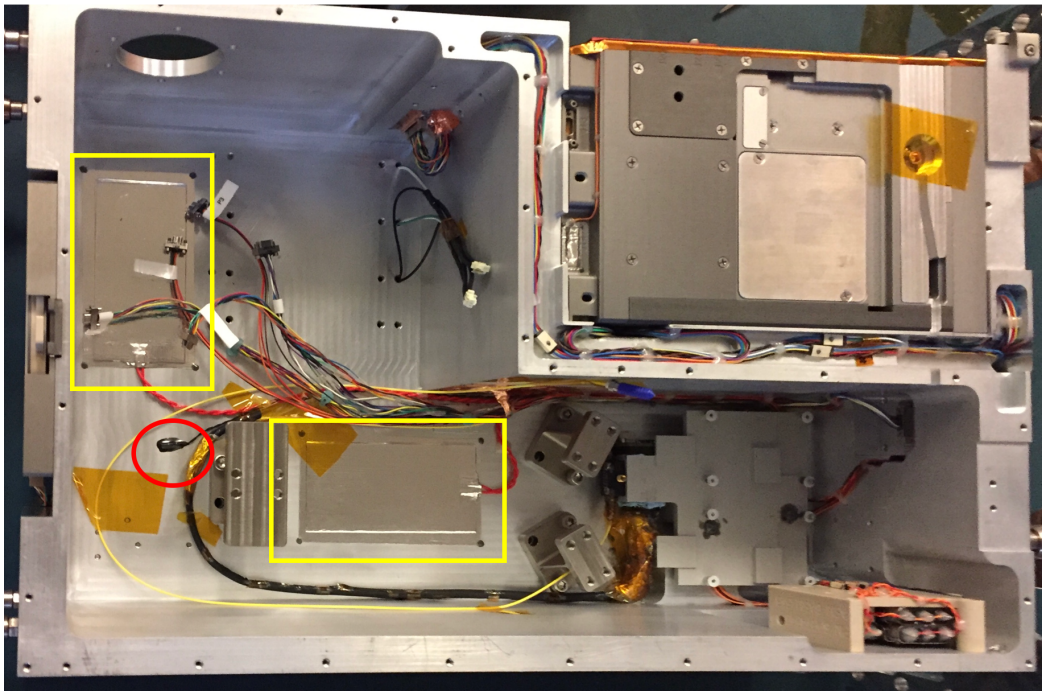

Figure 4-7: Payload/bus interface heater and temperature sensor location. The yellow rectangles indicate the location of the two kapton heaters and the red circle indicates the location of the temperature sensor.

out the mission. The blue points represent times when the payload heaters were in operational mode and the red points represent survival mode. The X's represent heater off points and the dots represent heater on. The operating mode heater setpoints are shown in blue at 15 °C on and 20 °C off. The survival mode heater setpoints are shown in red at 10 °C on and 15 °C off. From the available data, the interface temperature does not drop below 0 °C at any point and seems to remain at or below 20 °C. Additionally, the heaters are on in operating mode for a majority of the available data. Similarly to the optical bench thermal management performance, the interface heaters are never on above the corresponding heater operating mode setpoints.

Figure 4-9 shows the payload/bus interface temperature plotted with solar illumination and beta angle respectively. In this case, thermal variations due to eclipse status of the spacecraft may have more of an effect on the temperature. However, with limited data it is hard to say for sure. Since the heaters are on for a majority

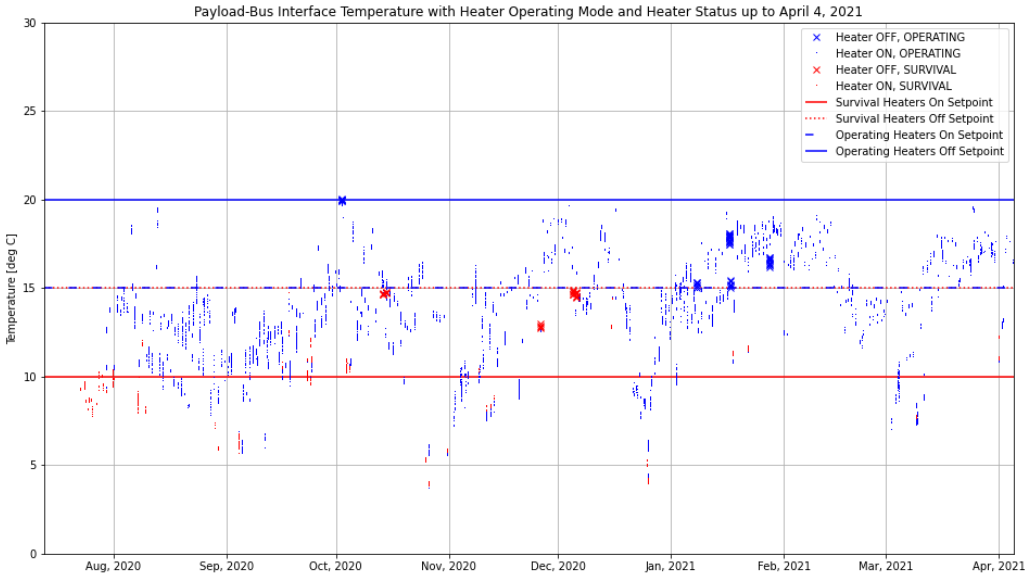

Figure 4-8: Payload/bus interface temperature over the mission duration plotted with heater status and operating mode. Heater setpoints for each operating mode are also shown. The blue points represent periods of operating mode and the red points represent periods of survival mode. The X's represent heaters off and the dots represent heaters on. The operating mode heater setpoints are shown in blue with the on setpoint at 15 °C and the off setpoint at 20 °C. The survival mode heater setpoints are shown in red with the on setpoint at 10 °C and the off setpoint at 15 °C.

of this dataset, they can be thought of as a constant heat source and so most of the temperature variations likely come from orbital configuration changes, or thermal discharge from spacecraft electronics.

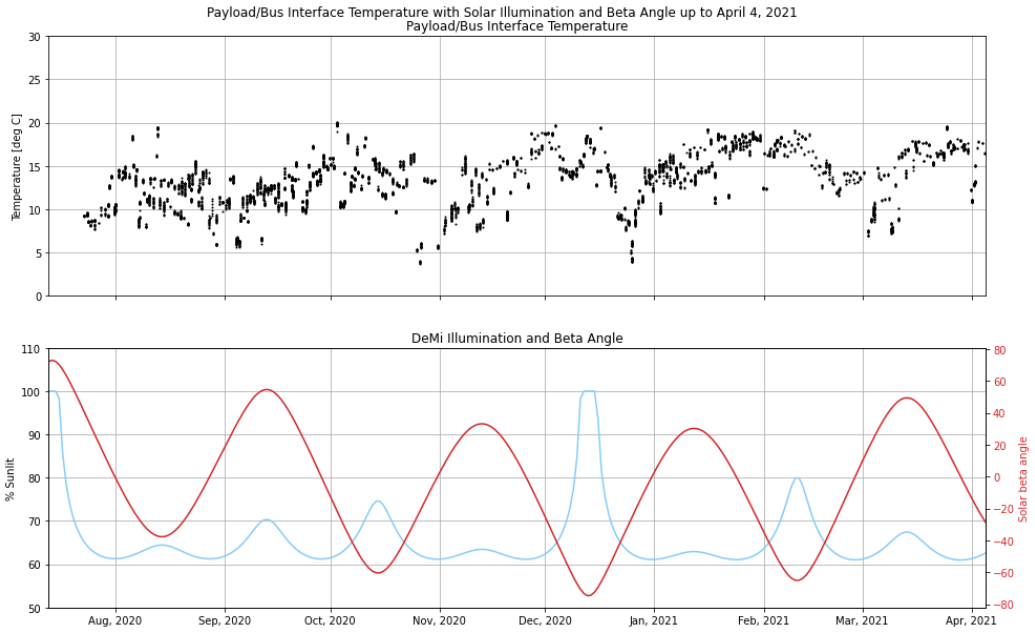

Figure 4-9: Payload/bus interface temperature shown as the black points in the top subplot. The bottom subplot shows the beta angle (red) in degrees and the percentage of an orbit that DeMi is illuminated by the sun (light blue).

4.3 Electric Power System

The electric power system (EPS) on the DeMi spacecraft is responsible for providing power to all of the spacecraft and payload components. The EPS consists of a battery, two solar panels, and a power routing board with voltage lines at 3.3 V, 5 V, 8 V, and 12 V.

The battery holds a maximum charge of 12.9 V based on design documents, but an observed maximum of 12.4 V. Figure 4-10 shows both the battery voltage and the battery current draw, along with spacecraft orbit percent sunlit and beta angle. Voltage is plotted in blue on the left axis and current is plotted in orange on the right. The battery current is positive when the battery is being discharged, and is

negative when the battery is being charged by the solar arrays. The received on-orbit spacecraft data indicates that battery voltage has never gotten over 12.4 V and has never gone under 11.5 V, staying within the battery power requirements. Additionally, the periods of negative current seem to align well with the periods of full power in the batteries and the periods of positive current align well with periods of decreased battery state of charge.

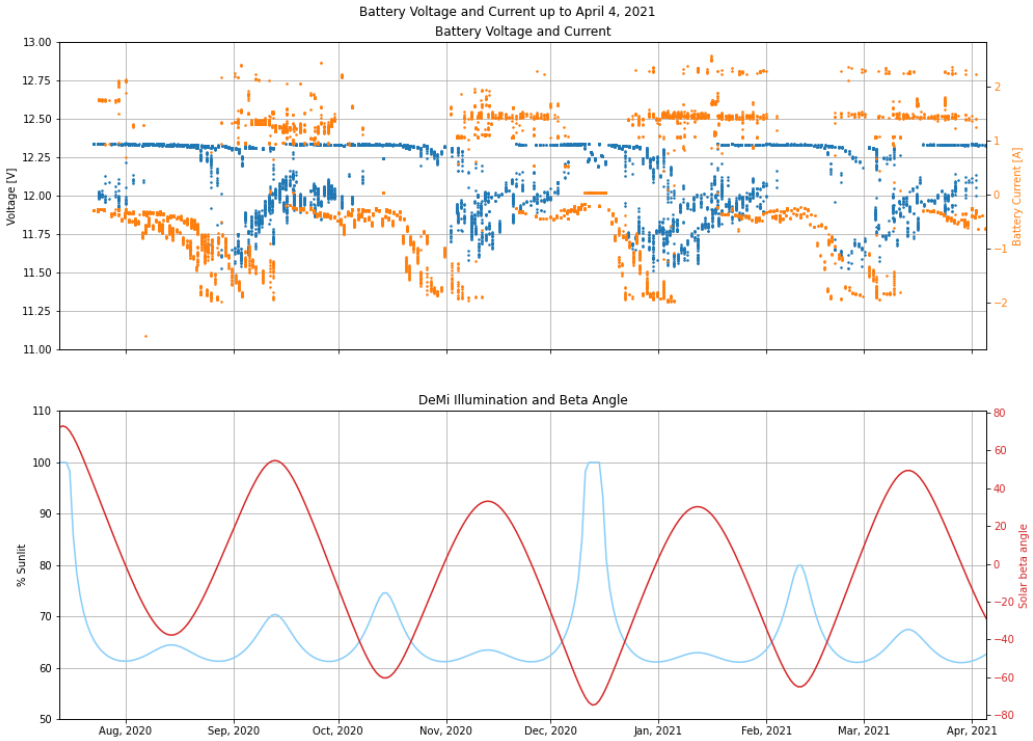

Figure 4-10: Battery voltage and current over mission duration. Battery voltage is plotted in blue in the top plot with the left axis indicators. Battery current is shown in orange with the right axis indicators. The bottom subplot shows the beta angle (red) in degrees and the percentage of an orbit that DeMi is illuminated by the sun (light blue).

In addition to charge level constraints, the batteries operate under thermal constraints. In order to safely charge, the batteries must remain between 0 °C and 45 °C. To safely discharge, the batteries must remain between -20°C and 60 °C. Figure 4-11 shows battery temperatures over the current mission lifetime. The battery temperature has stayed well within the tighter temperature range of 0 °C to 45 °C throughout the received mission data.

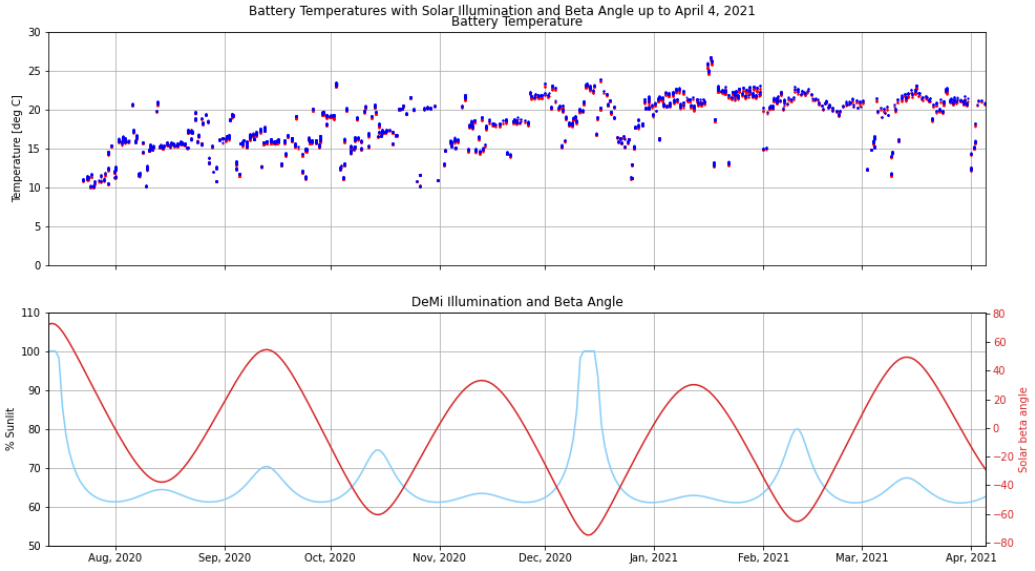

Figure 4-11: Battery temperatures in the top subplot. The bottom subplot shows the beta angle (red) in degrees and the percentage of an orbit that DeMi is illuminated by the sun (light blue).

Finally, the unregulated spacecraft voltage is shown in Figure 4-12 with battery voltage for reference. When the solar arrays are facing the sun and the spacecraft is charging, the unregulated spacecraft voltage reads in the 19 V range. When the spacecraft is operating on battery, the unregulated spacecraft voltage should match the battery voltage.

4.4 Radio

As discussed in Chapter 2, there are two radios on the DeMi CubeSat: the Cadet and the Lithium. The Cadet is the high data rate UHF radio that interfaces with the NASA Wallops Flight Facility (WFF) ground station. The Lithium is a UHF radio that interfaces with the MIT ground station. Unfortunately, temperatures from the Lithium radio are not available in the spacecraft data. There is, however, a history of Cadet temperatures on orbit that are shown in Figure 4-13. Cadet radio temperatures look normal with the exception of one data point from January 19, 2021, when the temperature data shows 307 °C. It is possible that during the

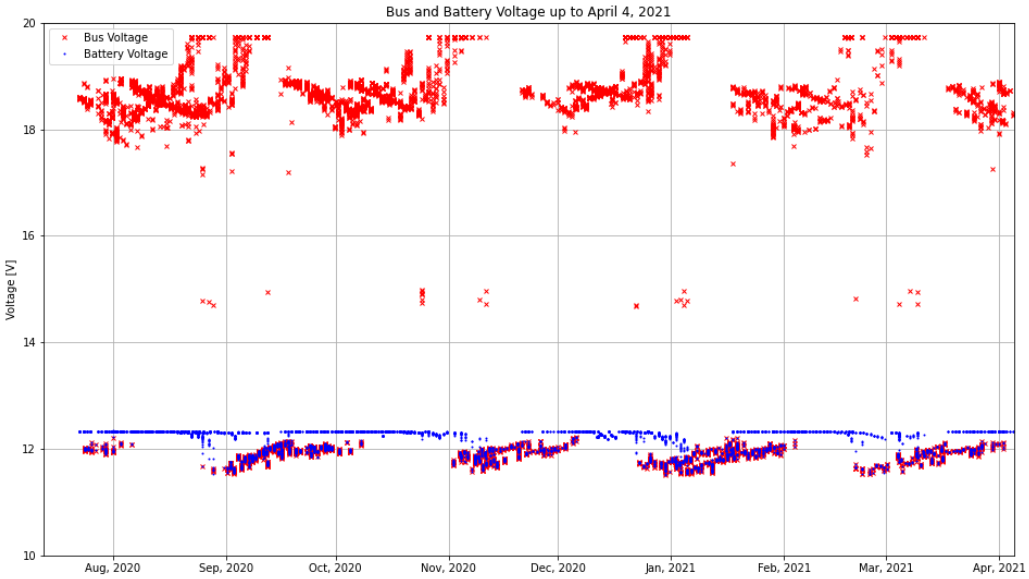

Figure 4-12: Bus voltage through April 4, 2021 shown with battery voltage for reference. The periods of higher voltage (in the 19 V range) are periods when the solar arrays are facing the sun and the periods of lower voltage (in the 12 V range) are when the spacecraft is operating off of battery power.

conversion of the raw data to the temperature values, an error occurred. However, the team has been unable to locate exactly what caused the anomalous value. Because temperature measurements directly before and directly after this anomalous point show temperatures in the 30's, this outlier is likely not a major cause for concern.

Zooming in on the temperature range between 10 °C and 40 °C, the fluctuations of Cadet temperature are more visible. Figure 4-14 shows these fluctuations along with solar illumination and beta angle.

4.5 Attitude Determination and Control Systems

The attitude determination and control system (ADCS) components are primarily used for orienting the satellite appropriately. This is to help processes like spacecraft battery charging and pointing at targets for external observations. The DeMi team has attempted several pointing operations, but has yet to take full advantage of the ADCS system on DeMi by taking observations of external targets.

Many of the commands to point the satellite, as well as many of the telemetry

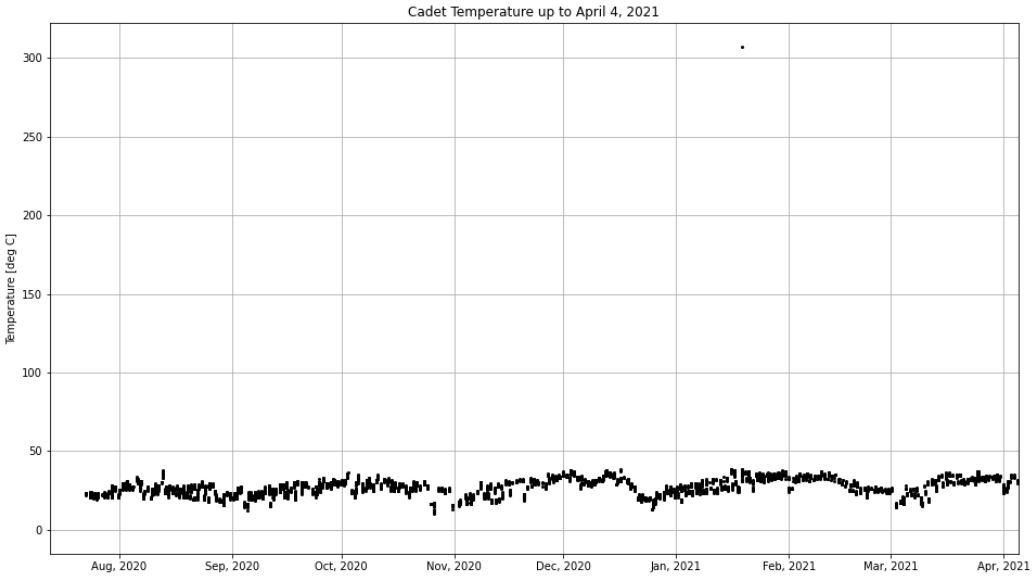

Figure 4-13: Cadet radio temperature history. Temperatures remain between 10 °C and 40 °C for all of the mission data except one anomalous point on January 19, 2021 where it is recorded as 307 °C.

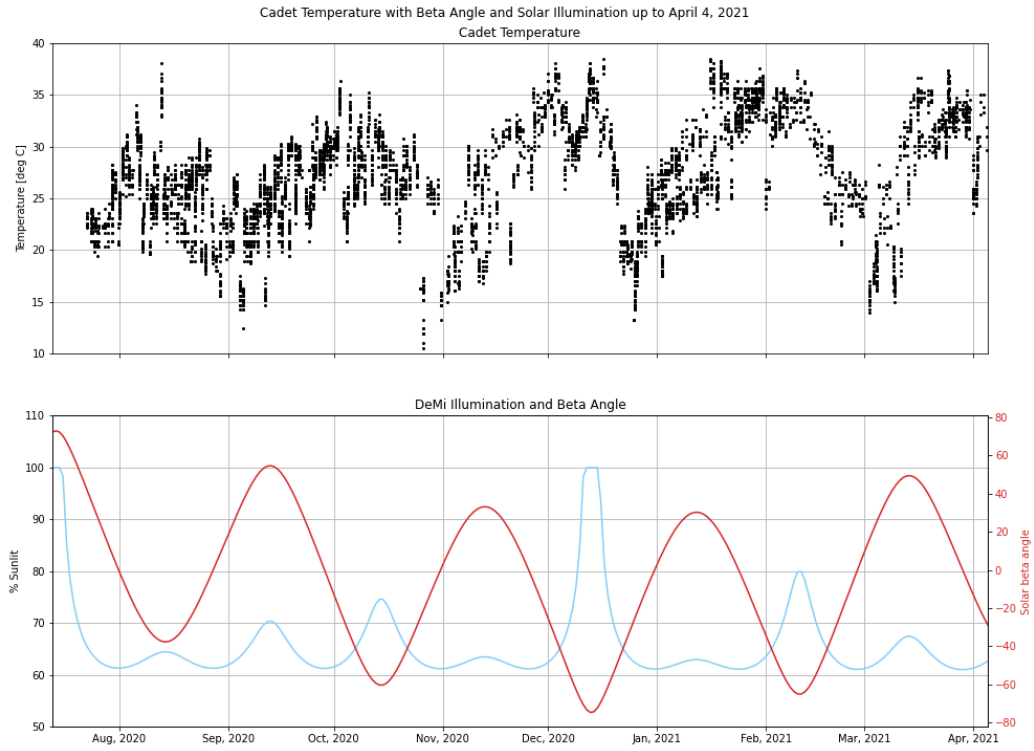

Figure 4-14: Cadet radio temperature shown in the top subplot. The bottom subplot shows the beta angle (red) in degrees and the percentage of an orbit that DeMi is illuminated by the sun (light blue).

items that capture how the spacecraft is pointing and moving, are given in terms of the spacecraft body frame. Figure 4-15 shows how the spacecraft body frame coordinate system is oriented relative to the satellite.

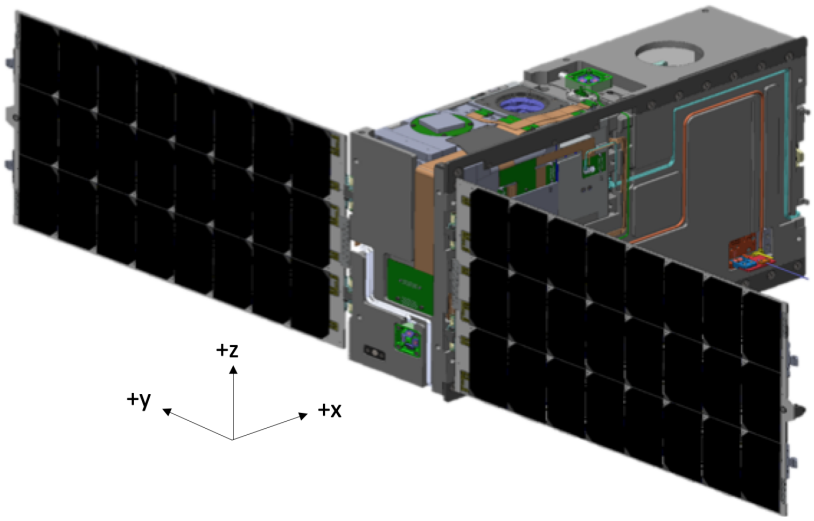

Figure 4-15: Spacecraft body frame. +x is from the solar panel plane into the satellite. +z is the face of the satellite with the payload and star tracker aperture. Image courtesy of Blue Canyon Technologies and adapted from [8].

4.5.1 Components

The BCT bus is equipped with a suite of ADCS components to detumble the spacecraft upon deployment and point the spacecraft in the desired configuration. These components include 3 reaction wheels, a star tracker, 3 packages of 4 sun sensor diodes, an inertial measurement unit (IMU), a GPS, a three-axis magnetometer, and 3 torque rods.

Reaction Wheels

One of the main components used to orient the spacecraft is the set of reaction wheels. The DeMi spacecraft has three reaction wheels and their speeds in rotations per minute over the mission are shown in Figure 4-16. In addition to showing reaction wheel speeds, the figure shows the periods where the spacecraft was commanded to

point by the operators. Many of the big jumps in speed correspond to pointing commands given by the operations team.

Figure 4-17 shows the reaction wheel drag along with the commanded pointing periods. Measuring the drag is a good way to understand reaction wheel performance degradation throughout the mission. In DeMi's case, the wheel drag has remained fairly low and relatively stable throughout the mission. The highest wheel drag seen to date is around $65\,\mathrm{rad\,s^{-2}}$. We would start to be concerned if drag estimates were in the 100's range for a long period of time. Furthermore, the drag only remained at elevated levels for a short period of time.

Looking at the reaction wheel temperatures, shown in Figure 4-18, we can see a harsh and persistent temperature jump between February 10th and March 2nd, 2021. During this period, the temperature data jumped up to around 100 °C and 80 °C. Despite close analysis of the February 9th data, the author has been unable to find a reason for this jump in temperature. Interestingly, this behavior is also present for all of the other ADCS component temperatures, shown in Figures 4-19 and 4-20. All of the temperature readings that showed this anomalous behavior go through the same A/D converter, so it is likely that the temperature jump was not representative of the true temperatures during this period. Furthermore, the anomaly appears to resolve itself on March 2nd, which corresponds to an observed bus reset. This reset likely cycled whatever was causing the false readings. Section 4.6 contains more information on the observed bus resets throughout the mission.

Star Tracker

The DeMi spacecraft uses a star tracker to measure its orientation and provide critical information to the ADCS components. Figures 4-19 and 4-20 show the star tracker detector temperature and star tracker baffle temperature respectively. Each is also plotted with solar illumination and beta angle in subplots. Just like with the reaction wheel temperatures, the star tracker temperatures also display the anomalous increase in temperature from February 10th and March 2nd, 2021.

Figure 4-21 shows the star tracker mean background brightness level, or back-

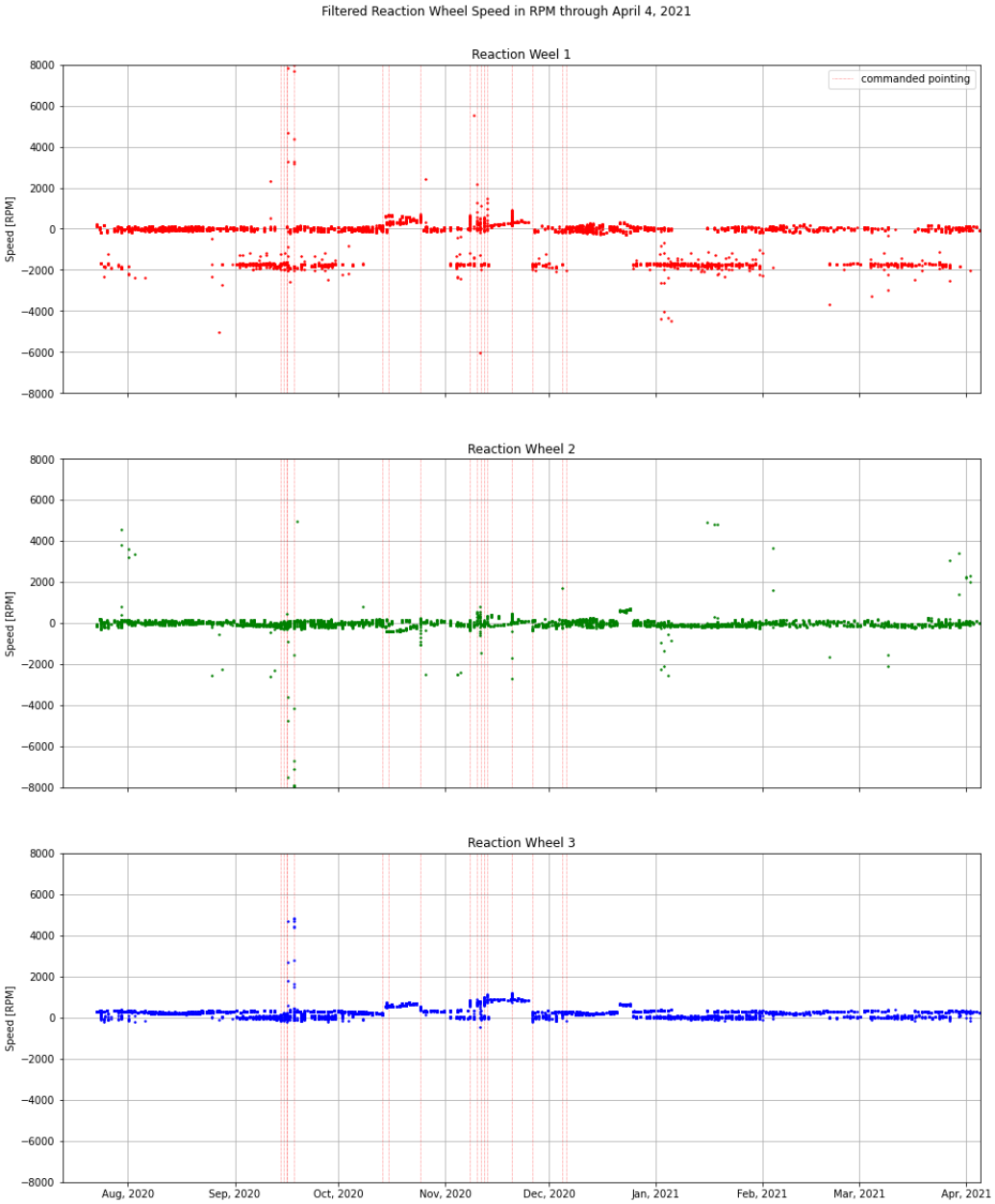

Figure 4-16: Reaction wheel speed given in RPM over the mission, shown with commanded pointing periods as the dotted red vertical lines.

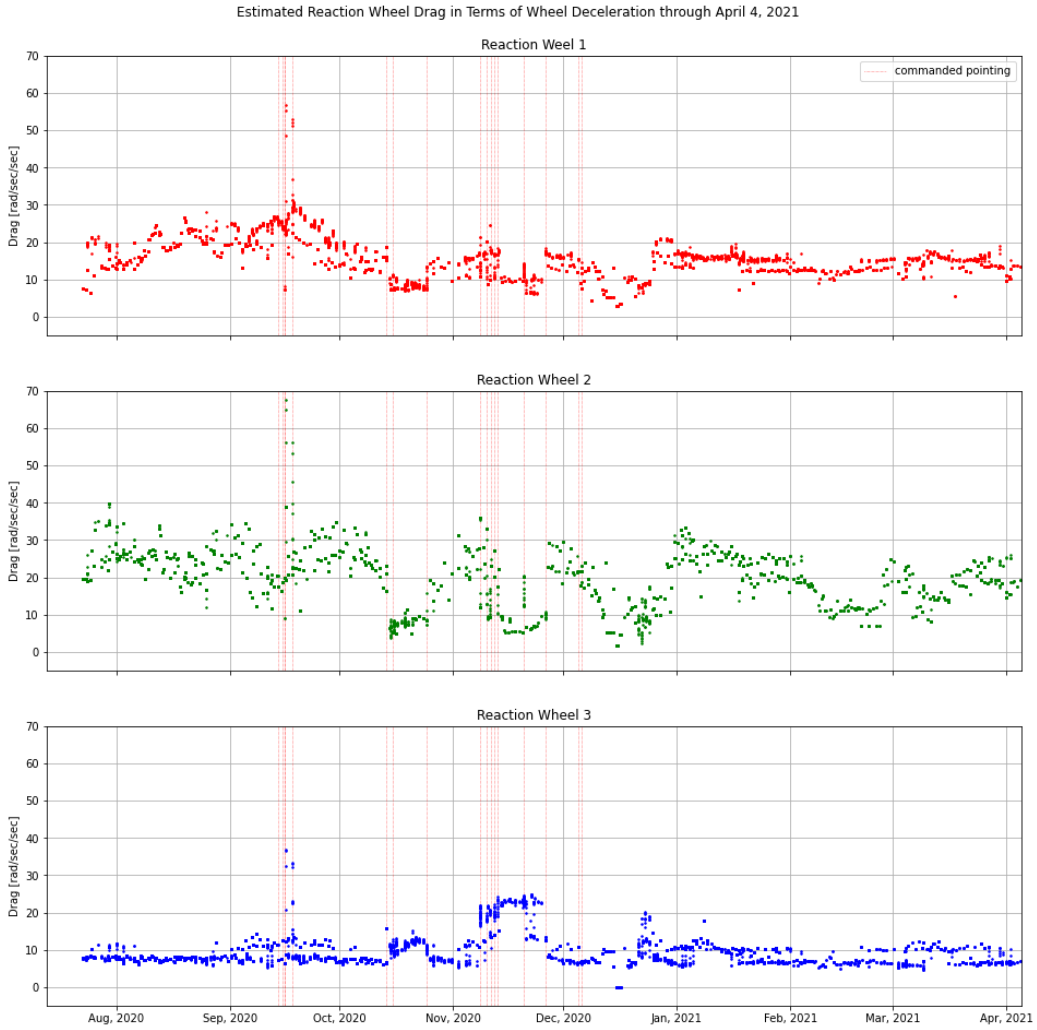

Figure 4-17: Reaction wheel drag with commanded pointing periods shown as the dotted red vertical lines.

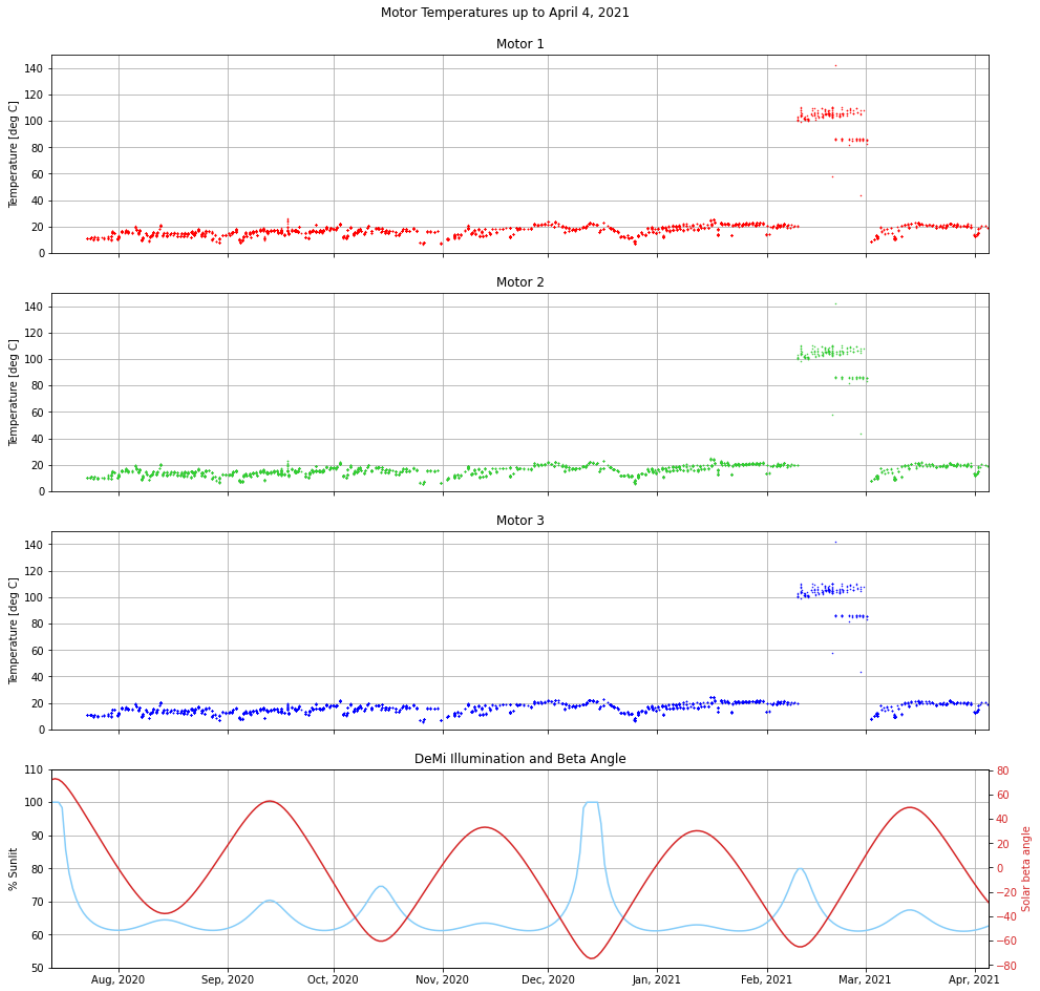

Figure 4-18: Reaction wheel temperatures shown in the top subplot. The bottom subplot shows the beta angle (red) in degrees and the percentage of an orbit that DeMi is illuminated by the sun (light blue).

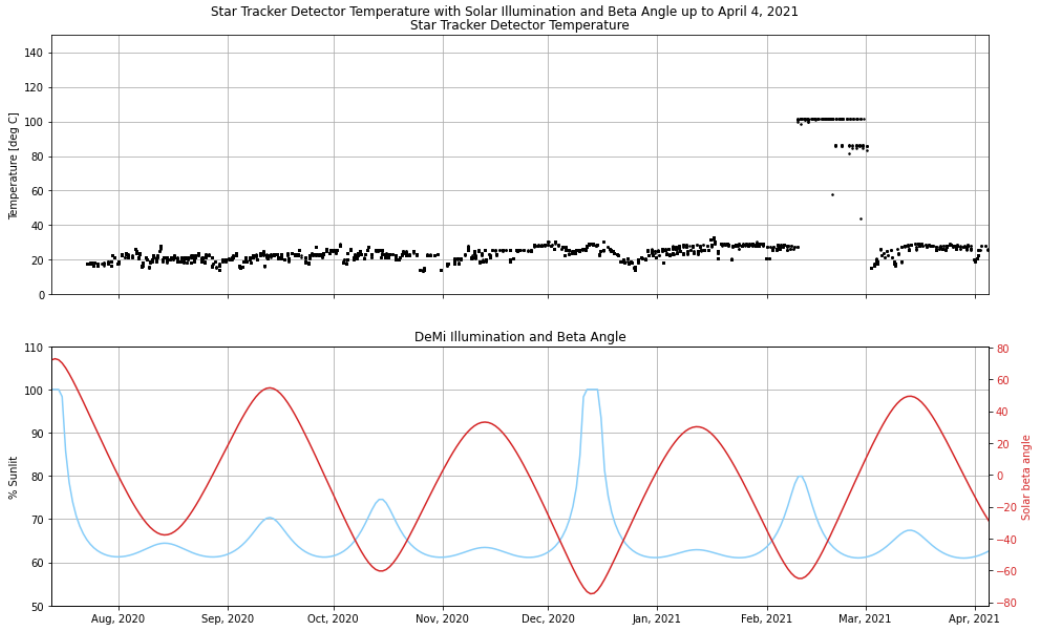

Figure 4-19: Star tracker detector temperature in the top subplot. The bottom subplot shows the beta angle (red) in degrees and the percentage of an orbit that DeMi is illuminated by the sun (light blue).

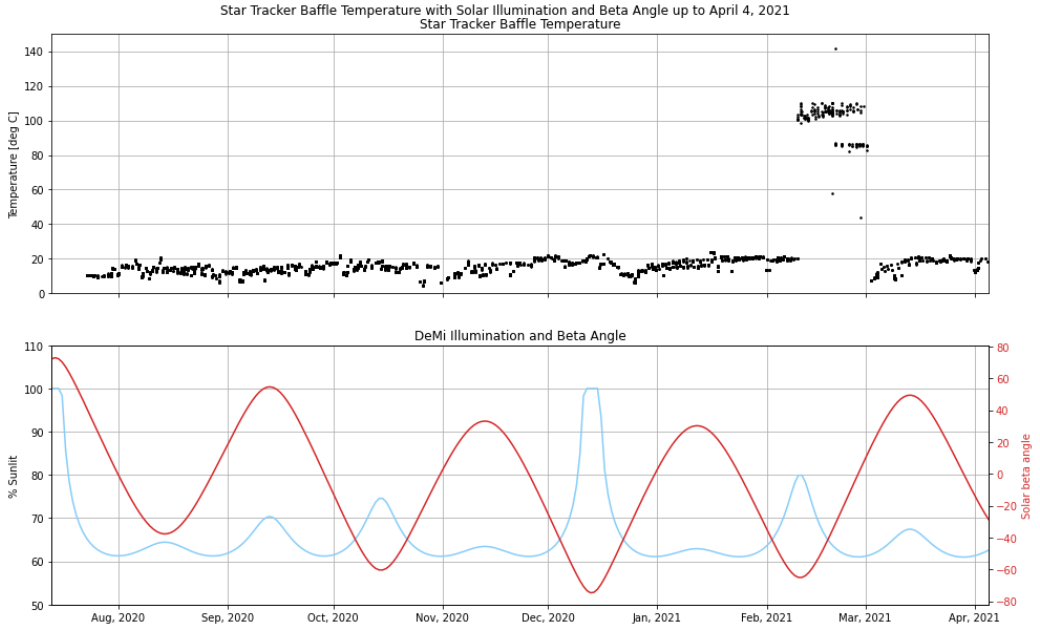

Figure 4-20: Star tracker baffle temperature in °C shown as the black dots. The bottom subplot shows the beta angle (red) in degrees and the percentage of an orbit that DeMi is illuminated by the sun (light blue).

ground noise level, plotted with detector temperature. The saturation point for the star tracker is at 1023 counts and is shown as the dashed horizontal gold line. For a majority of the DeMi mission, the median star tracker background level has remained below 200 counts, and there is no significant trend upwards in the median levels.

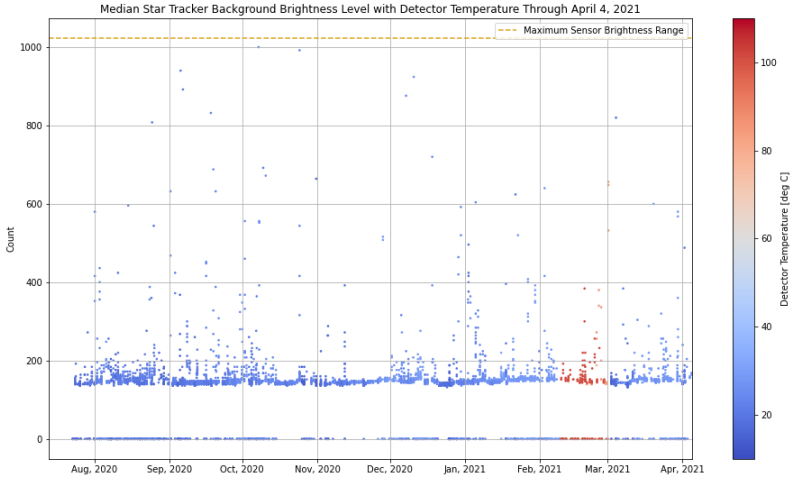

Figure 4-21: The median mean star tracker background brightness level plotted with detector temperature as the color. The horizontal dotted gold line is the saturation point for the star tracker detectors as 1023 counts.

Finally, Figures 4-22, 4-23, and 4-24 show star tracker estimates of spacecraft orientations and motions throughout the mission. These plots show estimated quaternions, RA and declination, and rate estimates respectively.

Sun Sensors

The DeMi satellite is equipped with 3 packages of 4 sun sensor diodes. The sun sensors help to provide coarse pointing information by measuring the amount of light hitting each of the diodes. Sun sensor package 1 is on the -X face of the spacecraft, package 2 is on the -Z face, and package 3 is on the +Z face. See Figure 4-15 for clarification on spacecraft orientation. Figure 4-25 shows all of the sun sensor diode illuminations. This is raw data from each diode shown in counts.

Figure 4-26 shows each sun sensor diode individually along with beta angle and

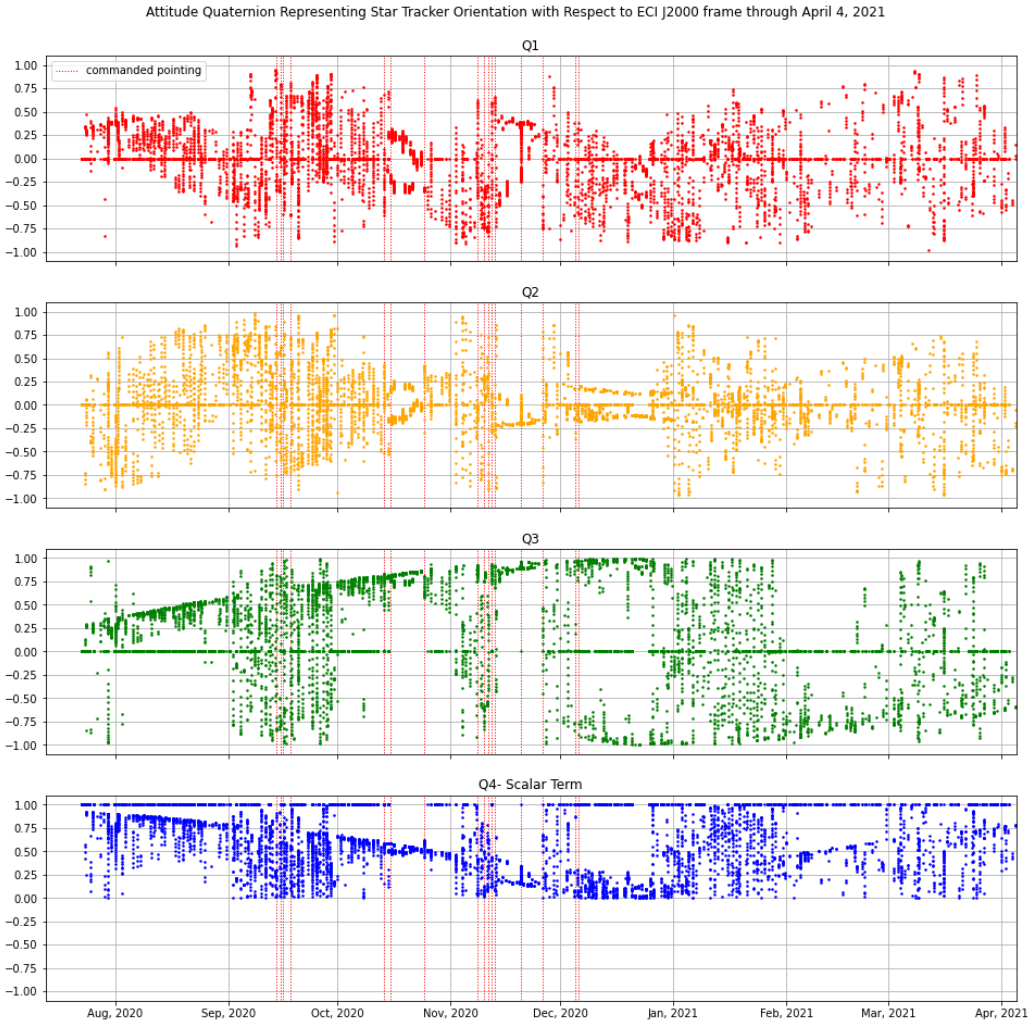

Figure 4-22: Star tracker estimated quaternions where Q4 is the scalar term. The red dashed vertical lines show commanded pointing attempts.

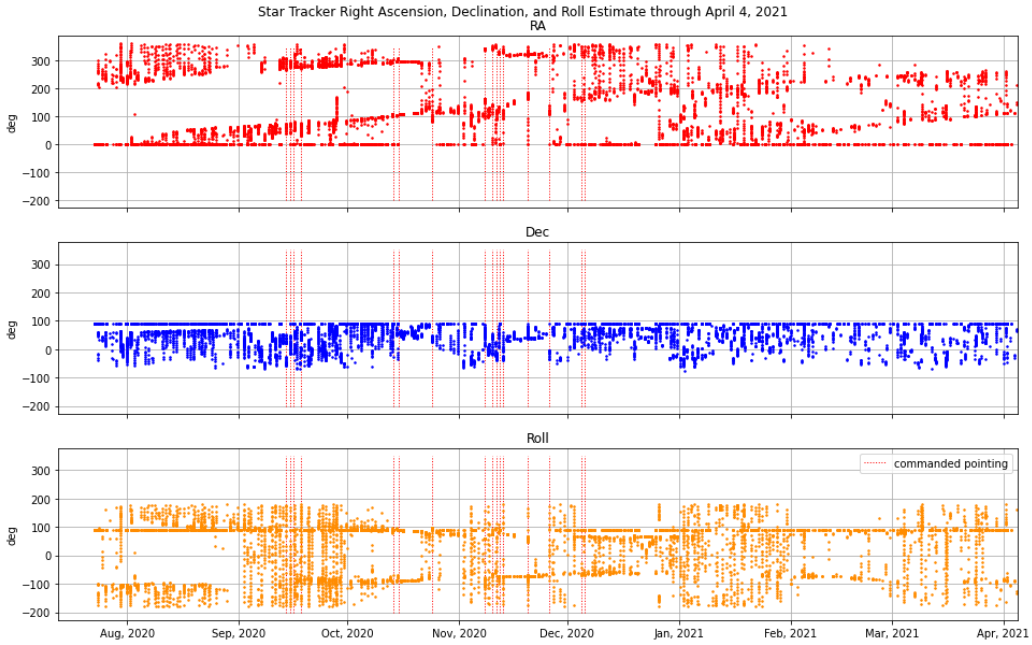

Figure 4-23: Star tracker estimated right ascension, declination, and roll. The red dashed vertical lines show commanded pointing attempts.

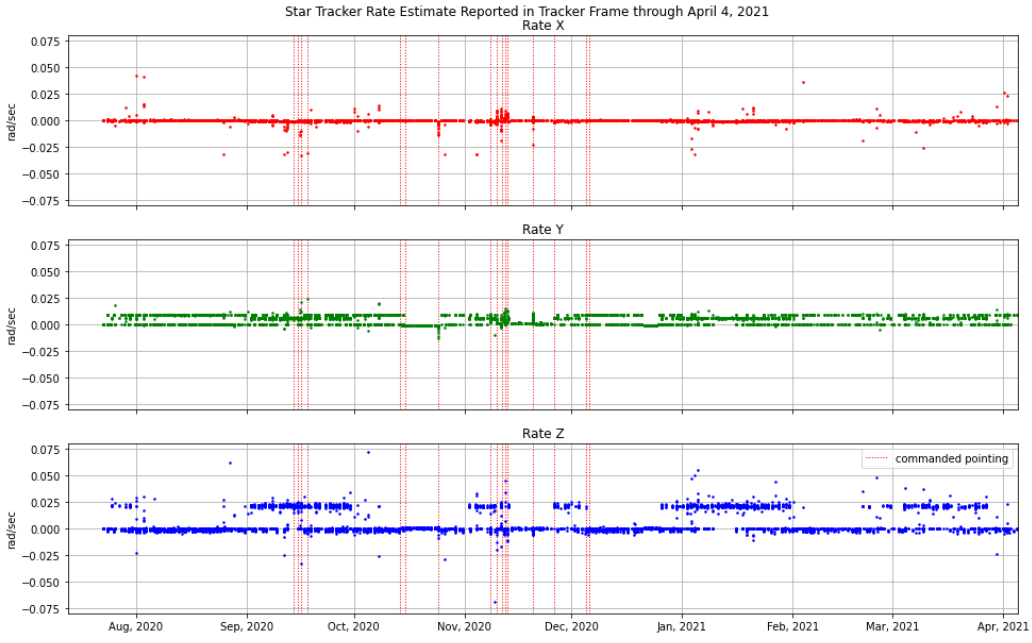

Figure 4-24: Star tracker estimated rates for X, Y, and Z in the spacecraft body frame. The red dashed vertical lines show commanded pointing attempts.

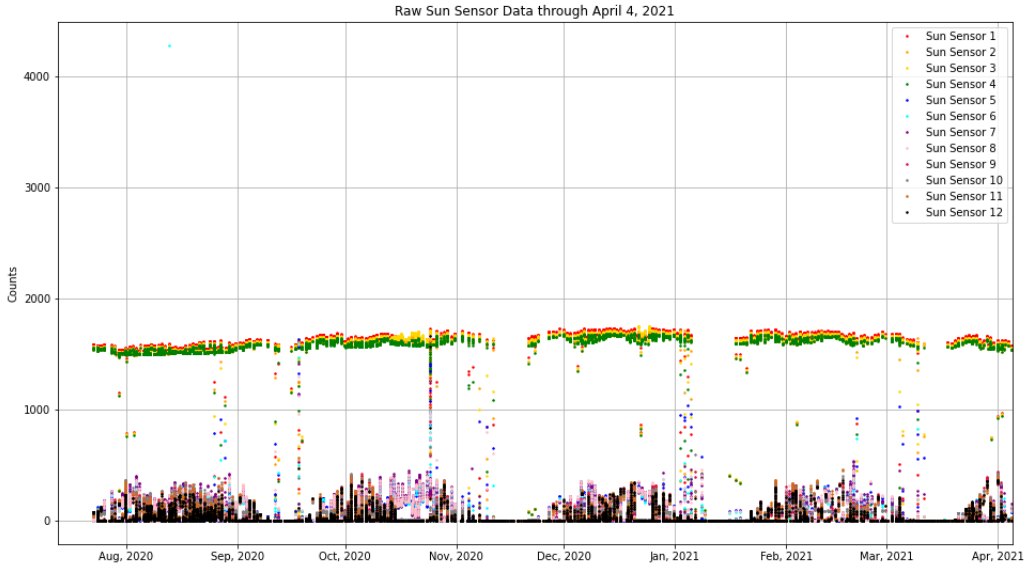

Figure 4-25: Raw sun sensor data for all sun sensor diodes.

solar illumination in the bottom subplot. Diodes 1-4 belong to package 1, 5-8 belong to package 2, and 9-12 belong to package 3. The diodes in each individual package appear to follow similar patterns to the rest of the diodes in the package.

With the raw sun sensor diode data, the spacecraft determines how many diodes are actually seeing the sun based on the counts reaching a threshold value. Figure 4-27 shows the breakdown of the number of diodes per package that are being used at a given time on the spacecraft. The maximum is 4 and the minimum is 0. Package 1 frequently observes the sun from all 4 diodes, which makes sense because this is the sun sensor package that faces the same direction as the solar panels. Package 3 is on the same face as the external aperture for the payload and the star tracker, so it should ideally never observe the sun. From the received spacecraft data, sun sensor package 3 only saw the sun two times, which were after a commanded pointing attempt. For this specific pointing attempt, we can confirm that the spacecraft oriented itself such that the sun was within the payload FOV keepout.

The sun sensors are also used to estimate the sun body vector. Figure 4-28 shows how accurate the vector is over time. A value of "GOOD" indicates that 3-4 diodes can see the sun, "COARSE" means 1-2 diodes see the sun, and "BAD" means that 0 diodes see the sun.

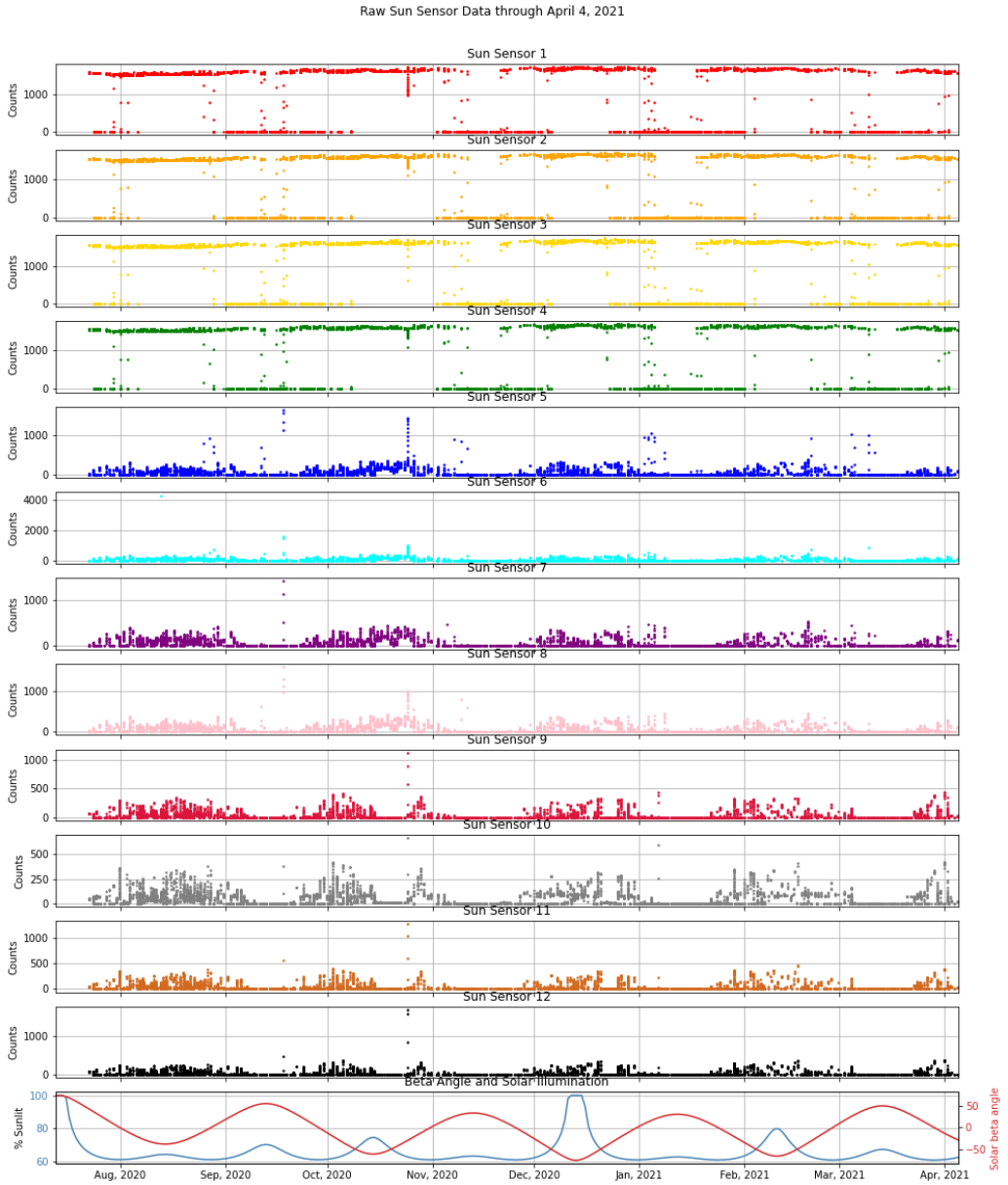

Figure 4-26: Raw sun sensor diode data from each of the 4 diodes in each of the three sun sensor packages. Sun sensor diodes 1-4 correspond to package 1, diodes 5-8 correspond to package 2, and diodes 9-12 correspond to package 3. The bottom-most subplot shows the beta angle (red) in degrees and the percentage of an orbit that DeMi is illuminated by the sun (light blue).

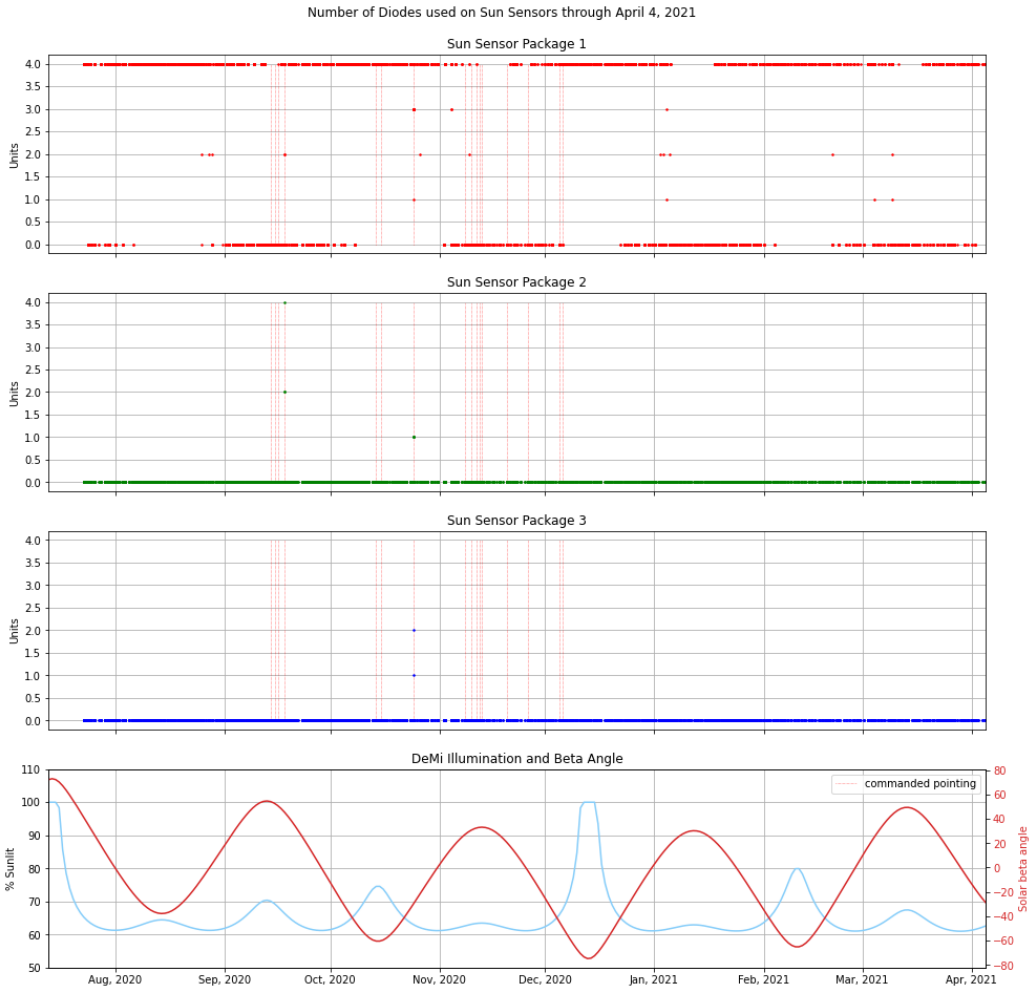

Figure 4-27: Number of diodes that "see" the sun per sun sensor package plotted with commanded pointing attempts.The red dashed vertical lines show commanded pointing attempts. The bottom-most subplot shows the beta angle (red) in degrees and the percentage of an orbit that DeMi is illuminated by the sun (light blue).

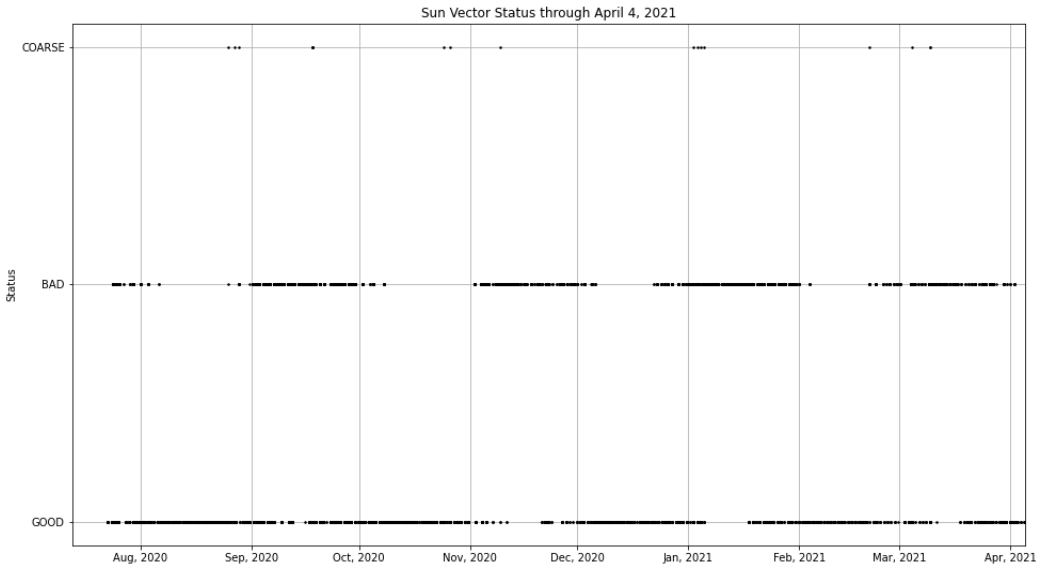

Figure 4-28: Sun vector status. This is an indication of how many diodes see the sun.

Finally, using data from the sun sensor diodes, the spacecraft can estimate the sun body vector. This estimation is shown in Figure 4-29.

Inertial Measurement Unit (IMU)

DeMi's inertial measurement unit (IMU) is another ADCS component used to estimate rates of motion in X, Y, and Z. Figure 4-30 shows these rate estimates along with commanded pointing attempts. These rates are similar to those estimated by the star tracker.

GPS

The GPS is used to confirm spacecraft position and to sync the onboard clocks. Figure 4-31 shows the times when the GPS information was valid, meaning GPS lock had been received within the last 90 seconds. In the early period of the mission, before the bus reconfiguration script in Appendix A was created, the operations team was not consistently enabling GPS, so the GPS information was not valid for a majority of the early operations. After November, however, the operations team made sure to re-enable the GPS after a reset of the spacecraft.

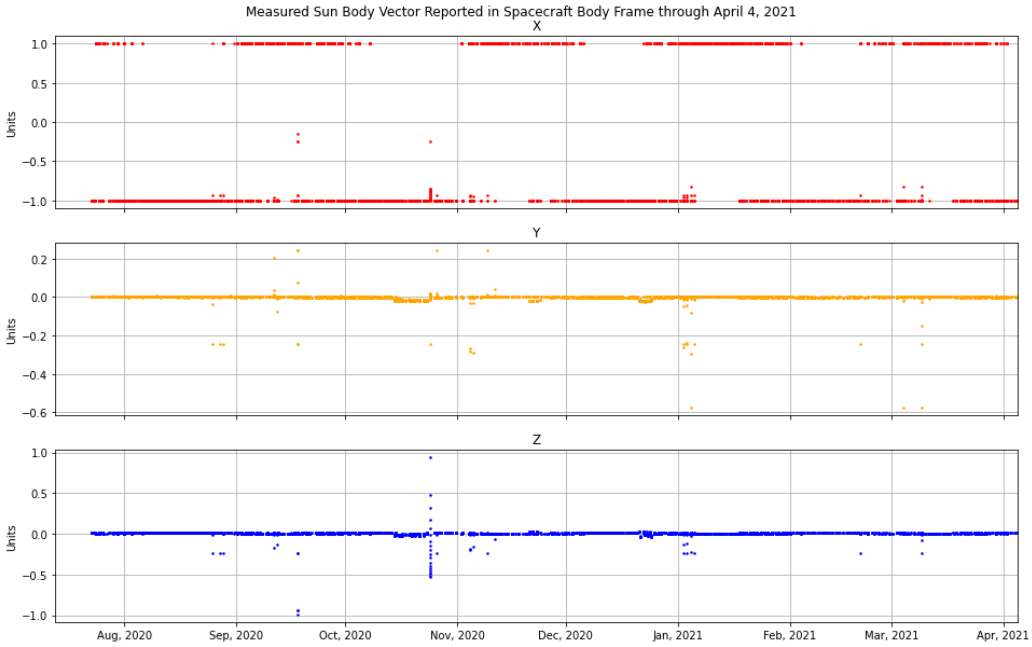

Figure 4-29: Sun body vector estimated from sun sensor data.

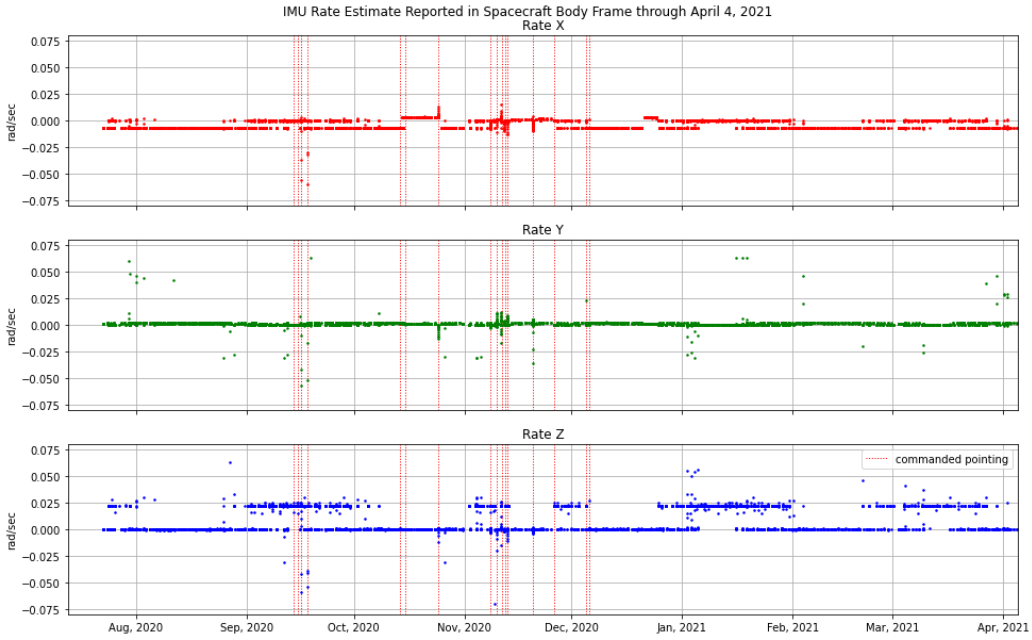

Figure 4-30: IMU rate estimates in radians per second for X, Y, and Z in the spacecraft body frame.

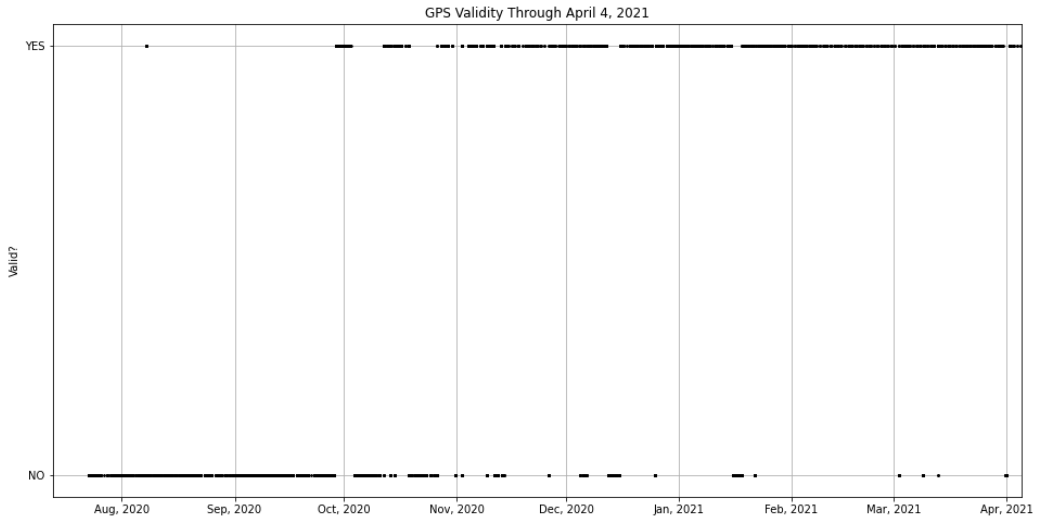

Figure 4-31: GPS validity.

Magnetometers

The ADCS system also consists of a magnetometer, which estimates the magnetic field in the spacecraft body frame. Figure 4-32 shows the estimated magnetic field vector based on magnetometer data. The data shown is relatively inconclusive and uninformative because only data from pass times have been collected and the data has not been compared to any magnetic field model. Future work with MIT graduate student Nicholas Belsten will look at how the measured magnetic field compares to the world magnetic model (WMM) and how the various spacecraft components may be impacting the measured magnetic field.

Torque Rods and System Momentum

Throughout the duration of the mission, the 3 torque rods have been enabled and operating in automatic mode. The torque rods are used systematically to dump system momentum when needed as specified by the program requirements. The torque rods have not been actively commanded and should not be nominally commanded by the operators throughout the mission.

Figure 4-33 shows the total system momentum. The total spacecraft momentum is a very important measurement because over a threshold value, the ADCS can no

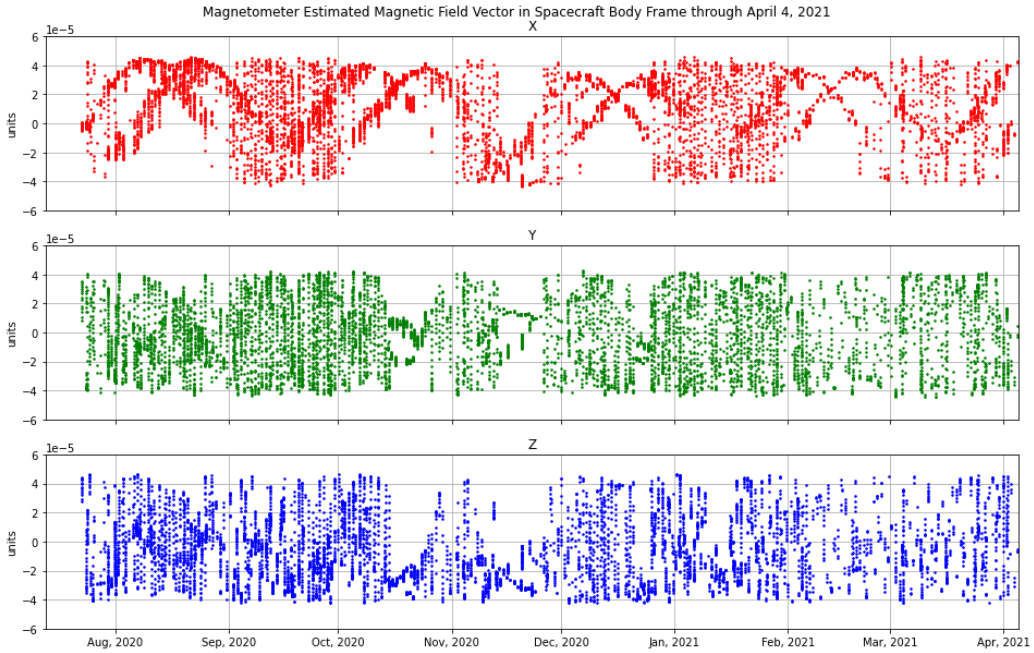

Figure 4-32: Estimated magnetic field vector in the spacecraft body frame based on magnetometer data.

longer perform attitude control of the spacecraft. The threshold for DeMi is set by the total momentum that a single reaction wheel can generate.

4.5.2 Pointing Attempts and Results

Payload Field of View Keepout

An issue that the DeMi team has been dealing with since initial contact is that the signal sometimes fades in and out during a pass. We think that this is due to the spacecraft roll, which is intended to keep the satellite thermally balanced and equally heated from the sun. While the rotation is necessary for the satellite, sometimes it causes the antennas to roll away from the ground station during passes. This causes the signal to weaken or even disappear for a bit of time. Because our passes are only typically on the order of only 10 minutes, the time lost due to roll can be significant. To try and combat these effects, the team has tried to send pointing commands to the satellite to actively point the antennas at the ground station for the duration of the pass and then go back to pointing the solar arrays at the sun.

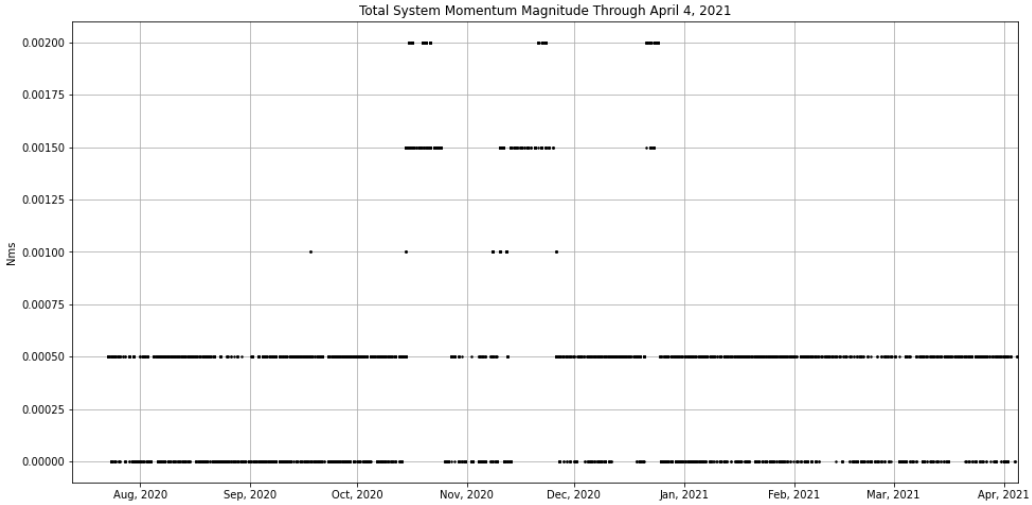

Figure 4-33: Total system momentum in Nms. The system momentum is dumped by the torque rods when it exceeds threshold value.

For many of these attempted ground station points, the satellite has gone into safe mode shortly after the command is executed. It took the team a while to understand why the pointing commands were not resulting in perfect passes, but ultimately it was discovered that the satellite was orienting such that the sun entered the payload field of view (FOV) keep out zone, which is 30° from boresight. When the sun enters the FOV keepout, the FOV keepout event check is triggered, which puts the satellite into safe mode and points the solar arrays back at the sun. Section 4.7 goes into more detail on event checks. Figure 4-34 shows the total number of times the FOV keepout event check was triggered along with the commanded pointing. Event check state of 1 indicates that the event check is enabled. This means that the spacecraft is actively checking that a condition is or is not met. In this case, the event check is checking that the sun remains outside of the 30° keepout angle from the payload boresight. An event check state of 0 indicates that the event check is disbled. When the FOV event check is triggered, meaning the sun is within the specified keepout zone, the event check state goes from 1 to 0. As is evident in the figure, every time the event check was triggered, or the state switched from 1 to 0, the operations team had commanded spacecraft pointing. This further confirms that the pointing commands sent by the DeMi team were causing the spacecraft to orient itself in a non-ideal way. For this

reason, the process for spacecraft pointing will need to be altered so as to not trigger this event check.

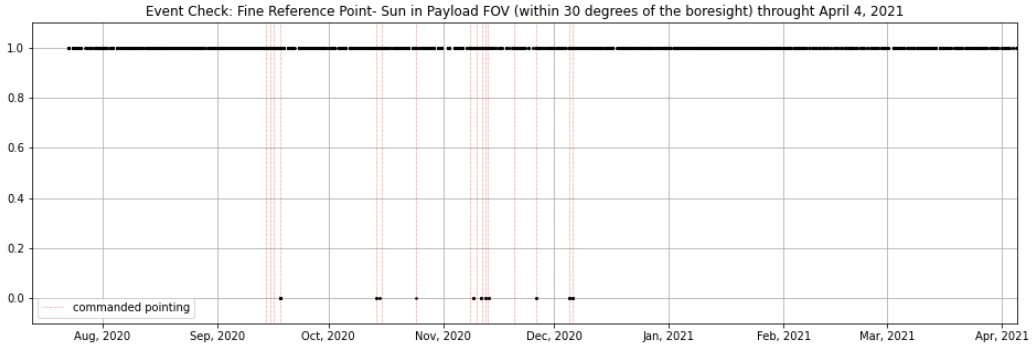

Figure 4-34: Sun in payload FOV keepout event check. The red dashed vertical lines show commanded pointing attempts. The triggering points are when the status changes from 1 to 0. A state of 1 means the event check in enabled, a state of 0 means the event check is disabled.

Currently, the team is working on resolving the commanded pointing issue by exploring a few ideas. One idea that we are looking into is being more explicit about the rotation about each axis on the spacecraft. MIT graduate student Patrick McKeen is actively working on this problem. Another idea, that we may use instead of or in conjunction with the explicit rotation, is to disable the payload FOV keep out event check while doing these commands. A keepout angle of 30° for the payload is very conservative and we do not plan on taking any images during the pointing. These two methods, and any other ideas that may come up, will be tested on the engineering model with simulated spacecraft behavior before trying it on the actual spacecraft.

Overall Spacecraft Pointing

Some of the plots throughout this chapter have included red dotted vertical lines to indicate commanded pointing. This is when the DeMi operators have sent up commands for DeMi to point itself. So far, the DeMi team has mainly been trying to point the satellite such that the antennas on board face in the optimal direction for passes. Figure 4-35 shows the spacecraft ADCS mode over time with an overlay of the pointing commands. Many of the pointing command periods overlap or appear to trigger the "FINE_REF_POINT" mode, which is where the spacecraft is performing

fine pointing to a target. The "SUN_POINT" mode is where the solar panels are facing the sun. "SUN_POINT" is the default ADCS mode for the spacecraft and is entered after a safe mode is triggered.

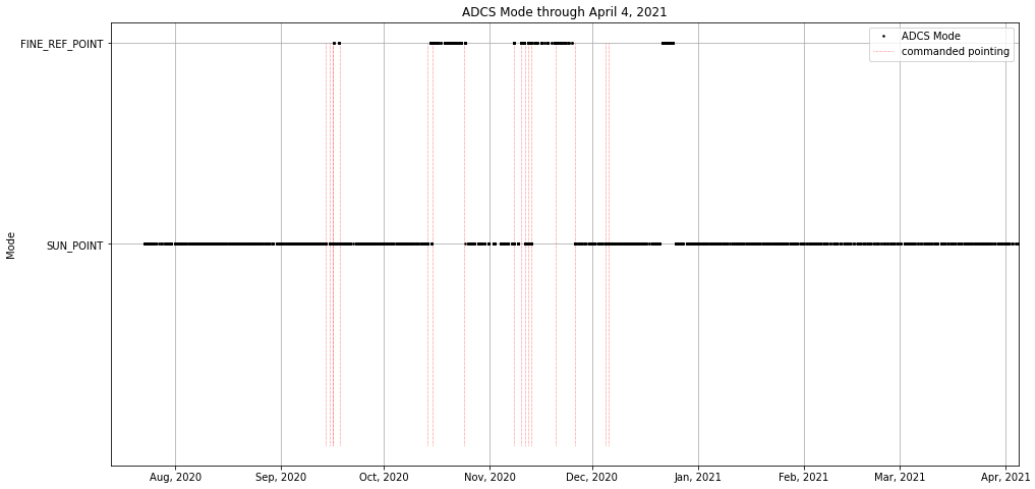

Figure 4-35: Spacecraft ADCS mode with pointing command periods requested by the operations team. FINE_REF_POINT is when the spacecraft is actively pointing at a target, such as the ground station, and SUN_POINT is the default state where the solar panels are pointed at the sun.

Figures 4-36, 4-37, and 4-38 show the commanded attitude quaternions, the commanded rates in degrees per second, and the commanded acceleration respectively along with the periods of commanded pointing attempts. Once again, the pointing attempts correspond to many of the changes in the quaternions, rates, and accelerations.

4.6 Bus Resets

Between deployment in July and April 4th, 2021, the DeMi spacecraft has experienced 17 bus resets. A few of these resets have been commanded, many others have been due to South Atlantic Anomaly (SAA) radiation strikes, and others have been caused by undetermined anomalies. Table 4.1 shows the dates and causes of all of the resets through April 4, 2021. Figure 4-39 shows the bus resets throughout the mission. The black dotted lines are the high rate run counts which represent how long the flight

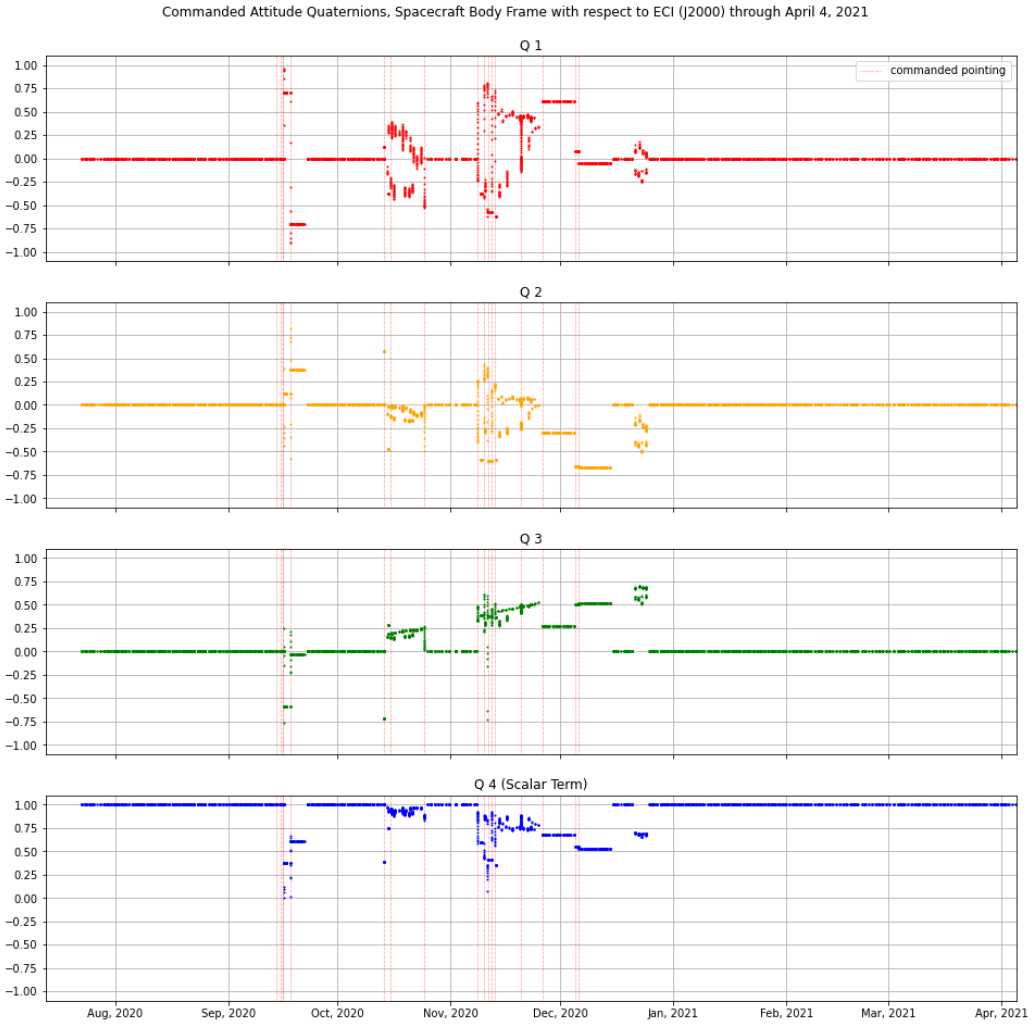

Figure 4-36: Commanded attitude quaternions. The red dashed vertical lines show commanded pointing attempts. Q4 is the scalar term and is always positive.

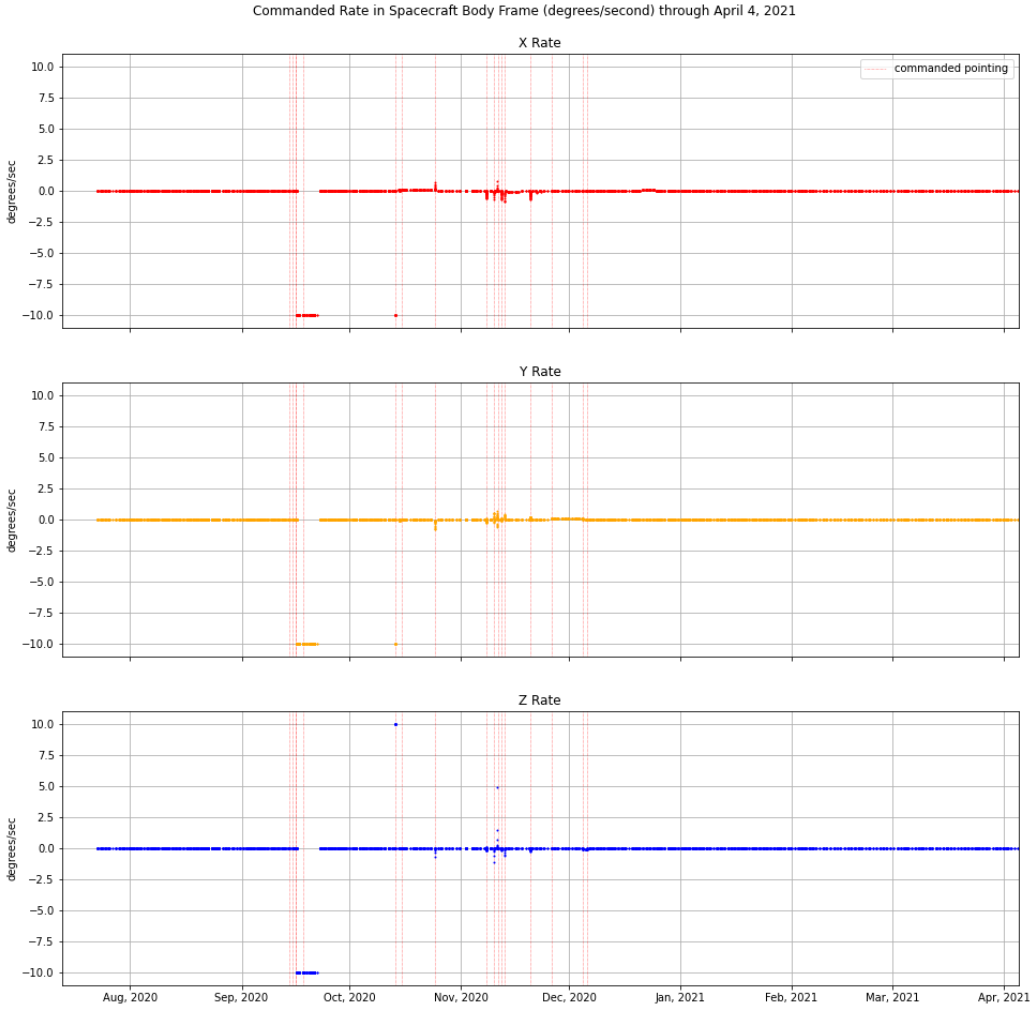

Figure 4-37: Commanded x, y, and z acceleration. The red dashed vertical lines show commanded pointing attempts.

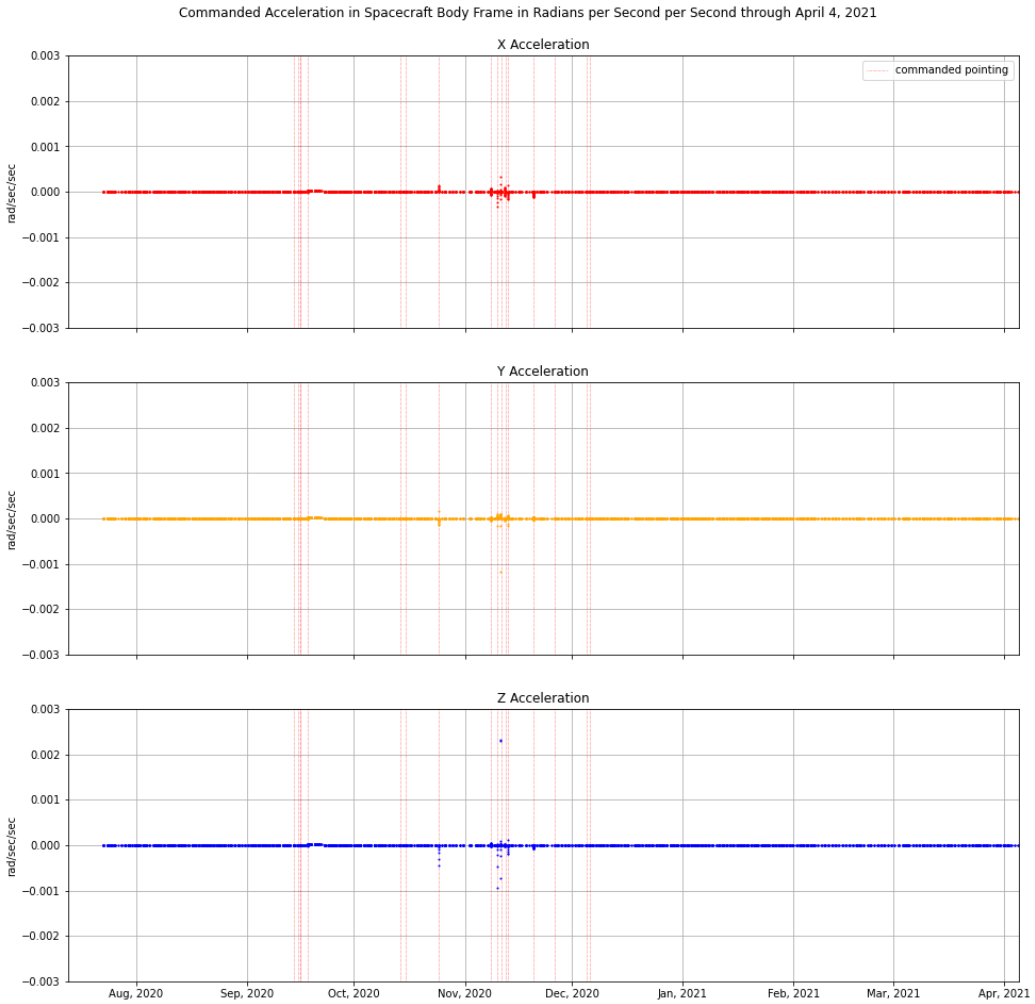

Figure 4-38: Commanded x, y, and z rates. The red dashed vertical lines show commanded pointing attempts.

software has been running. Every time the bus is reset, shown by the pink vertical lines, the run count starts back at 0.

Date of Reset	Reason for Rest
7/31/20	commanded
8/7/20	unknown cause
8/9/20	unknown cause
8/28/20	commanded
9/4/20	unknown cause
9/23/20	unknown cause
9/24/20	unknown cause
10/3/20	unknown cause
10/25/20	SAA
10/31/20	SAA
12/15/20	SAA
12/25/20	SAA
1/17/21	SAA
1/21/21	SAA
3/2/21	SAA
3/9/21	SAA
3/31/21	unknown cause

Table 4.1: Table of the dates of bus resets between July 13, 2020 and April 4, 2021. May of the resets were due to South Atlantic Anomaly (SAA) radiation strikes, a few were commanded resets, and the others have undetermined causes.

When the bus resets occur, the bus and payload heaters get set to survival, the spacecraft points the solar arrays at the sun, the Lithium radio beacons, the event checks get reset to their default state, and power to the payload gets cut. To automate and standardize the reconfiguration process of the satellite, meaning to turn on the heaters, re-enable the appropriate event checks, and enable certain spacecraft operations, the author wrote a script that takes all of the reconfiguration actions. This script can be found in Appendix C.

4.7 Event Checks

Some of the DeMi spacecraft fault protection is defined by a list of event checks. Event checks are conditions that, when enabled, are constantly being checked by the

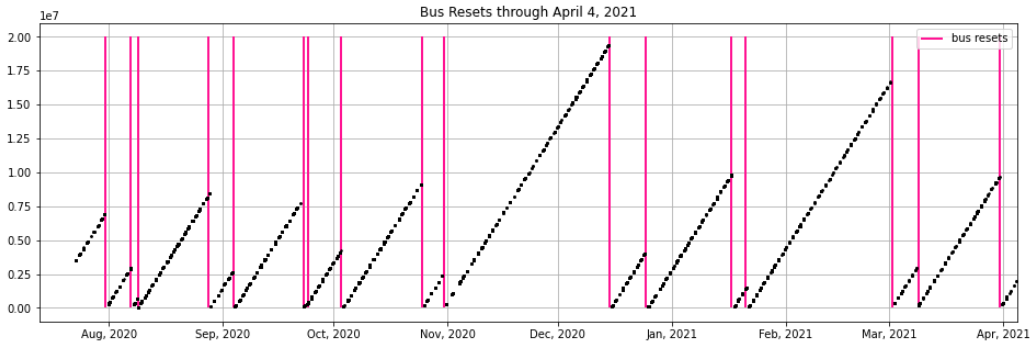

Figure 4-39: Bus resets, shown as the pink vertical lines, and high rate run count of the flight software, shown as the black dotted lines. The high rate run count is run by the flight software and is reset to 0 every time the software (or bus) reboots.

spacecraft. If the condition is not met, the spacecraft will take an action to resolve the issue, reset the spacecraft, or put the spacecraft into safe mode. DeMi has 26 defined event checks that cover temperature limits, voltage limits, battery state of charge, radio lockup, loss of communication, sun in the payload FOV, and booting the payload to the appropriate flight computer and SD card. The DeMi-specific event checks are shown in Table 4.2. Some of the event checks have been added to the same row as similar event checks because they are checking the same telemetry item, but respond differently. Those different responses are designated by "OR" in the Response When Triggered column.

Event Check	Response When Triggered
Cadet radio lock-up	Cadet radio power cycle
Sun in payload FOV	Transitions to safe mode
Payload 1 or Payload 2 communication stops	Transitions payload to safe mode OR to shutdown
Check if payload 1 booted to SD card A/B	Cycle payload 1 power
Check if payload 2 booted to SD card A/B	Cycle payload 2 power
Payload temperatures out of operational bounds	Payloads to safe mode OR payloads power down
Payload temperatures out of survival bounds	Power down both payloads

Table 4.2: DeMi event checks to ensure fault tolerance during operations.

The only two event checks that have been triggered unexpectedly are the payload FOV event check, discussed in the pointing attempts section, and the Cadet radio lock-up event check. The cadet lock up event check is shown in Figure 4-40 along with bus reset periods. When the bus is reset for any reason, the Cadet lock up event check is disabled by default. Therefore, all of the points on the disabled (0) line that

correspond with the bus reset lines are not actual radio lockups. The period at the end of July to the beginning of August was a period of time when the DeMi team did not know that the event check needed to be re-enabled. After the beginning of August, once the team began regularly using the bus reconfiguration script, only 3 Cadet radio lockup events were present in the available data. One of them occurred in mid-August, one in mid-September, and one at the beginning of January.

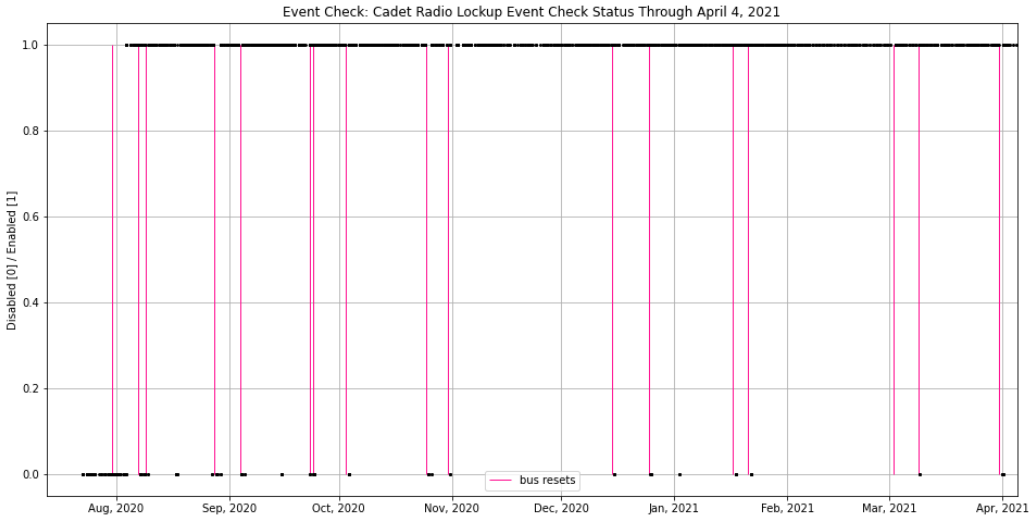

Figure 4-40: Cadet radio lockup event check with bus resets shown as the pink vertical lines. All of the points on the 0.0 line that come right after the pink bus reset lines are not actual event check triggers, they are just incidents of the event check reverting back to default state upon reset. The points in mid August, mid September, and early January do not align with observed bus resets and are possibly Cadet lockup events.

4.8 Overall Bus Health Discussion

Overall, the spacecraft is performing very well. All of the temperatures have remained within bounds, other than the anomalous offset experienced by the ADCS components. Additionally, the spacecraft is responding to pointing commands from the ground, however user error is causing safe mode triggers. These commanded pointing errors will be addressed by the DeMi team over the coming months. Additionally, all of the event checks are working as expected and performing the necessary functions to keep the spacecraft healthy and operational.

THIS PAGE INTENTIONALLY LEFT BLANK

Chapter 5

Results, Discussion, and Future Work

5.1 Results and Discussion

As discussed in Chapter 2, the NASA Wallops Flight Facility (WFF), which serves as DeMi's high data rate ground station, was offline for a majority of the mission duration to date. Luckily, as of the writing of this thesis, the WFF ground station is back online and the team was able to resume passes. With the project budget, we were allocated 100 passes from the WFF and we have used close to 50% of those allocated passes. During the time that WFF was not operational, the DeMi operations team made several modifications to the MIT campus ground station to supplement passes and work on receiving the larger files that would have been downlinked through WFF. These modifications are still in work and will continue to be useful because they allow the operations team to use the campus ground station for more than just monitoring spacecraft health.

In Chapter 3, payload on-orbit operations are discussed. MIT graduate student Rachel Morgan has confirmed that the payload has captured and returned several successful images that show the deformable mirror (DM), laser, and cameras are working. However, the successful images were taken early in the mission. After the WFF ground station went offline, the team was unable to downlink additional images and properly test the payload components. Since WFF came back online, the team has tried to capture more images to demonstrate successful operation of

all of the payload components, but those efforts have been unsuccessful. Now, the team is working on resolving issues with the deformable mirror by uplinking scripts to the payload that will record DM voltages to a file that the team can downlink through the WFF ground station. Additionally, the team is exploring options for attempting operations on the backup SD card or on the Payload 2 flight computer. Both cameras and the laser still appear to be working, however the DM commands have been unsuccessful since WFF returned to operations. The Raspberry Pi flight computer temperatures have been largely elevated and will be monitored more closely in the future.

Overall, the DeMi spacecraft bus, discussed in Chapter 4, remains healthy and operational. There have been no major anomalies, just a few minor issues with the radios, the payload FOV keepout during commanded pointing, and some anomalous temperature measurement data from the ADCS components. Payload temperatures have remained within operational bounds, and the batteries are charging and discharging as expected. The attitude determination and controls system (ADCS) is functioning appropriately and the team will likely be attempting more refined pointing attempts in the coming months. The spacecraft has experienced 17 bus resets from deployment on July 13th, 2020 through April 4, 2021. Many of these bus resets are likely due to radiation strikes from the South Atlantic Anomaly (SAA) region over South America.

5.2 Future Work

As of April 4, 2021, the DeMi mission has been operational for several months past the originally planned mission lifetime. The DeMi operations team has a lot of work ahead of them to try to meet all of the mission objectives and to keep all of the spacecraft and payload components operating nominally. The team will continue to monitor the telemetry items presented throughout this thesis and will continue to resolve problems as they arise.

5.2.1 Operations

Presently, the DeMi team's main focus is resolving the issues with the DM actuation. In order to successfully meet all of the mission's science objectives, the team needs to understand why the DM actuation attempts have been unsuccessful recently. The operations team is currently pursuing several paths for resolving the issue. The team is working on uploading scripts to the payload that will record power to the DM as it is turned on and actuated and will confirm that properly formatted commands are being sent to and received by the DM. These scripts will save those measurements to a file that the team can downlink to try to rule out any issues with the power supply or command formatting. Additionally the team may try to command DM actuation with the backup SD card, SD B, to see if that makes a difference. Finally, more research and analysis is being done on the Raspberry Pi behaviors at high temperatures, as discussed in reference to Figure 3-2 and 3-3. The team is looking through environmental testing data and performing more ground testing with a Raspberry Pi and the engineering model of the payload.

After the DM issue is resolved or understood completely, the next priority is to get the commanded pointing working without triggering the payload field of view (FOV) keep out event check. Testing is currently being done on the engineering model with a simulated spacecraft to try to recreate some of the event check triggering we were seeing in orbit and then correct it. It is possible that the pointing commands should be more explicit and specify rotation of all the axes to actively avoid getting the sun in the keepout zone. This is work that is currently being done by MIT graduate student Patrick McKeen. Another option that the team is considering is disabling the event check for the FOV keepout while we attempt pointing the radios toward the ground station. This should be done only if prior analysis is done to ensure that the payload FOV is not stuck facing the sun for the duration of the pass.

Finally, some of the modifications that the team made during the WFF downtime need to be uploaded to the Payload 2 computer and the backup SD cards. The team is working on uploading these "fixes" periodically and in parallel with some of the

troubleshooting discussed above. Some of the fixes are necessary for carrying out all of the testing that needs to be done.

The operations team is testing these changes in as flight-like of a configuration as possible on the engineering model. However, due to configuration differences, the team has so far been unable to connect or simulate a Payload 2 flight computer.

5.2.2 Telemetry Analysis

As for the telemetry analysis, future work is likely to include more analysis of the temperature anomaly seen in Figure 4-13 of the Cadet radio temperature data set. This analysis will help confirm that the anomaly was not representative of true temperatures and give insight into where the issue originated. Additionally, the team may try to better understand the cause of the anomalous ADCS component temperature offset from February, 2021 so that the behavior can be prevented in the future. More analysis of the magnetometer data and the satellite's impact on measured magnetic field is planned with the help of MIT graduate student Nicholas Belsten. There is also more work to be done to understand the state of health of the bus electronics, including timing, GPS locks, and stored command processing. Finally, more analysis will be done on space weather throughout the mission and how that might have had an impact on some of the telemetry presented here, including bus resets with unknown causes.

Appendix A

List of Acronyms

ADCS: Attitude Determination and Control System

AO: Adaptive optics

BMC: Boston Micromachines Corporation

CalPoly: California Polytechnic State University

CAD: Computer-aided design

C&DH: Command and Data Handling

CMOS: Complementary metal-oxide semiconductor

ConOps: Concept of operations

DeMi: Deformable Mirror Demonstration Mission

DM: Deformable mirror

EPS: Electric Power System

FOV: Field of View

FSW: Flight Software

IMU: Inertial Measurement Unit

ISS: International Space Station

MEMS: Microelectromechanical systems

MIT: Massachusetts Institute of Technology

OAP: Off-axis parabolic mirror

PSF: Point spread function

RF: Radio Frequency

SAA: South Atlantic Anomaly

SHWFS: Shack-Hartmann wavefront sensor

SOH: State of Health

STAR Lab: Space Telecommunications, Astronomy and Radiation Laboratory

TRL: Technology Readiness Level

TVAC: Thermal vacuum

WFF: Wallops Flight Facility

WFS: Wavefront sensor

WMM: World Magnetic Model

Appendix B

Beta Angle and Solar Illumination Script

```
# Script created by Joey Murphy and modified by Jenny Gubner for use in this thesis
import matplotlib.pyplot as plt
import matplotlib.dates as mdates
from skyfield.api import Topos, load, Time, EarthSatellite
from skyfield.nutationlib import iau2000b_radians
from skyfield.elementslib import osculating_elements_of
from skyfield.constants import ERAD
from numpy import count_nonzero, cos, sin, arcsin, degrees, average, sqrt, square, clip
from scipy.signal import savgol_filter
import datetime
import math

# Calculate the Solar beta angle for a satellite at time t (in degrees), and the corresponding
# proportion of sunlit time (expressed as a percentage).
def solar_beta(sat, sun, earth, t):
    sun_astro = earth.at(t).observe(sun)
    sun_ra, sun_dec, sun_distance = sun_astro.radec()
    elements = osculating_elements_of(sat.at(t))
```

```
19      inclination = elements.inclination.radians
20      raan = elements.longitude_of_ascending_node.radians
21      pre_beta = cos(sun_dec.radians) * sin(inclination) * sin(raan -
        sun_ra.radians) + \
22                  sin(sun_dec.radians) * cos(inclination)
23      beta = arcsin(clip(pre_beta, -1, 1))
24      sun_prop = sun_proportion(beta, elements)
25      return degrees(beta), sun_prop
26
27  # https://stackoverflow.com/questions/48235232/valueerror-math-domain-
        error-from-math-acos-and-nan-from-numpy-arccos
28  # For a given solar beta angle, return the corresponding theoretical
        proportion
29  # of time in sun per orbit
30  def sun_proportion(solar_beta, osc_elements):
31      sm_axis = osc_elements.semi_major_axis.m # in meters, consistent
        with ERAD
32      pre_sun = sqrt(1 - square(ERAD / sm_axis)) / cos(solar_beta)
33      pre_sun = clip(pre_sun, -1, 1)
34      return (0.5 + 1 / math.pi * arcsin(pre_sun)) * 100
35
36  ts = load.timescale(builtin=True)
37  TLE = open(path + "/demi_latest.txt").readlines()
38  satellite = EarthSatellite(TLE[1],TLE[2],TLE[0],ts)
39  eph = load(path + "/de421.bsp")
40  sun = eph['sun']
41  earth = eph['earth']
42  sunlit_by_days = []
43  solar_beta_by_days = []
44  solar_prop_by_days = []
45
46  #Set up Beta Angle Days
47  start_time = ts.utc(2020,7,13)
48  days = []
49  for i in range(1, 366):
50      next_day = ts.tt_jd(start_time.tt + i)
```

```
51      dayrange = ts.utc(*list(next_day.utc[:-1]),range(0,86400,10))
52      dayrange._nutation_angles = iau2000b_radians(dayrange)
53      illum_array = satellite.at(dayrange).is_sunlit(eph)
54      sunlit_pct = count_nonzero(illum_array) / len(illum_array) * 100.0
55      sunlit_by_days.append(sunlit_pct)
56      beta, sunprop = solar_beta(satellite, sun, earth, dayrange)
57      #if i % 10 == 0:
58          #print(i, beta[0], sunprop[0])
59      solar_beta_by_days.append(average(beta))
60      solar_prop_by_days.append(average(sunprop))
61      days.append(i)
62
63  # https://stackoverflow.com/questions/46633544/smoothing-out-curve-in-
        python
64  # https://en.wikipedia.org/wiki/SavitzkyGolay_filter
65  # https://stackoverflow.com/questions/20618804/how-to-smooth-a-curve-in-
        the-right-way
66  yhat = savgol_filter(sunlit_by_days, 7, 2) # window size, polynomial
        order
67  start = start_time.utc_datetime()
68  end = start + datetime.timedelta(days=365)
69  year_drange = mdates.drange(start, end, datetime.timedelta(hours=24))
```

THIS PAGE INTENTIONALLY LEFT BLANK

Appendix C

Bus Reset Reconfiguration Script

The script presented here has been modified to anonymize telemetry items.

```
######## Script to Re-Configure After Bus Reset #########
######## Written by Jenny Gubner, Sept 15, 2020 #########
######## Logic updated by Jenny on Sept 22, 2020 #########

######## Re-enable Event Checks A, B, C, D, E #########
# Taken from enable_event_checks.rb script
ecs_to_enable = [A, B, C, D, E]

for i in ecs_to_enable
  while(tlm("UUT EVENT_CHECK CHECK_ENABLED_PACK_BIT#{i}") == 0)
    start_cmd_count = tlm("UUT COMMAND_TLM RECEIVED_COUNT").to_i
    cmd("UUT ENABLE with NUM #{i}")
    while(tlm("UUT TLM COUNT").to_i < start_cmd_count +2 and tlm("UUT
    EVENT_CHECK CHECK_ENABLED_PACK_BIT#{i}") == 0)
        wait(1)
    end
  end
  p "Done enabling EC #{i}"
end

####### Turn on Cadet #######
```

```
# Taken from quick_health_check.rb and fsw_pl1_downlink_slow.rb
while not (tlm("UUT POWER CADET_8V") == "ON" and tlm("UUT POWER CADET_5V
    ") == "ON" and tlm("UUT POWER CADET_3V3") == "ON")
  start_cmd_count = tlm("UUT TLM COUNT").to_i
  cmd("UUT MACRO with ID A")
  while(tlm("UUT TLM COUNT").to_i < start_cmd_count +2 and (tlm("UUT
    POWER CADET_8V") == "ON" and tlm("UUT POWER CADET_5V") == "ON" and
    tlm("UUT POWER CADET_3V3") == "ON") == false)
     wait(30)
  end
  p "Done turning on Cadet"
end

####### Set Heater Config to Operational #########
# Taken from set_heater_setpoints.rb script and quick_health_check.rb
while not (tlm("UUT POWER HEATER_CONFIG1") == "OPERATING" and tlm("UUT
    POWER HEATER_CONFIG2") == "OPERATING")
  start_cmd_count = tlm("UUT TLM COUNT").to_i
  cmd("UUT HEATER_CONFIG with CONTROLLER_NUM A, CONFIG OPERATING")
  while(tlm("UUT TLM COUNT").to_i < start_cmd_count +2 and (tlm("UUT
    POWER HEATER_CONFIG1") == "OPERATING" and tlm("UUT POWER
    HEATER_CONFIG2") == "OPERATING") == false)
     wait(1)
  end
  p "Done setting heaters to operational"
end

# Turn on payload if within temperature bounds
# Not yet implemented


####### Re-Enable Stored Commands ########
#Taken from quick_health_check.rb and
stored_cmd_status = tlm("UUT TLM STORED_ENABLED")
while not tlm("UUT TLM STORED_ENABLED") == 'EN'
  start_cmd_count = tlm("UUT TLM COUNT").to_i
```

```
51    cmd("UUT STORED_CMD_ENABLE with ON_OFF ON")
52    while(tlm("UUT TLM COUNT").to_i < start_cmd_count +2 and tlm("UUT TLM
        STORED_ENABLED") != true)
53      wait(1)
54    end
55    p "Done enabling stored commands"
56  end
57
58  # Re-upload macro B
59  # Not yet implemented
60
61  # Re-Upload macro C
62  # Not yet implemented
63
64  # Disable Beacon if you feel it is safe
65  # Not yet implemented
```

THIS PAGE INTENTIONALLY LEFT BLANK

Bibliography

[1] Gregory Allan, Ewan S. Douglas, Derek Barnes, Mark Egan, Gabor Furesz, Warren Grunwald, Jennifer Gubner, Bobby G. Holden, Christian Haughwout, Paula do Vale Pereira, Abigail J. Stein, and Kerri L. Cahoy. The Deformable Mirror Demonstration Mission (DeMi) CubeSat: Optomechanical Design, Validation, and Laboratory Calibration. 2018.

[2] Gregory W. Allan. Simulation and Testing of Wavefront Reconstruction Algorithms for the Deformable Mirror (DeMi) Cubesat. Master's thesis, Massachusetts Institute of Technology, 9 2018.

[3] LLC Astronautical Development. *Li-2 User Manual*. Astronautical Development, LLC, rev. 0.1 edition, January 2017. http://www.astrodev.com/public_html3/datasheet/LithiumII-User_Manual_01122017.pdf.

[4] H.W. Babcock. The Possibility of Compensating Astronomical Seeing. *Publications of the Astronomical Society of the Pacific*, 65(386):229–236, 1953.

[5] Kerri Cahoy, Gregory Allan, Ayesha Hein, Andrew Kennedy, Lee Zachary, Erin Main, Weston Marlow, Thomas Murphy, Daniel Cousins, and William J. Blackwell. Integration and Test of the Microwave Radiometer Technology Acceleration (MiRaTA) CubeSat. Presented at the AIAA/USU Conference on Small Satellites, August 2017. https://digitalcommons.usu.edu/smallsat/2017/all2017/32/.

[6] San Luis Obispo California Polytechnic State University. 6U CubeSat Design Specification. Online, April 2016.

[7] P. do Vale Pereira, B. Holden, R. Morgan, J. Gubner, T. J. Murphy, C. Haughwout, G. Allan, Y. Xin, W. Kammerer, and K. Cahoy. Thermomechanical design and testing of the Deformable Mirror Demonstration Mission (DeMi) CubeSat. In *Proceedings of the AIAA/USU Conference on Small Satellites*, Science/Mission Payloads, 2020. SSC20-III-06. https://digitalcommons.usu.edu/smallsat/2020/all2020/121/.

[8] Paula do Vale Pereira. Thermomechanical design and testing of the Deformable Mirror (DeMi) CubeSat. Paper presented at the AIAA/USU Conference on Small Satellites, 2020.

[9] Jennifer N. Gubner. Deformable Mirror Demonstration Mission. Bachelor‘s thesis, Wellesley College, December 2018.

[10] Alexander C. Haughwout. Electronics development for the Deformable Mirror Demonstration Mission (DeMi). Master's thesis, Massachusetts Institute of Technology, 2018.

[11] P.-Y. Madec. Overview of Deformable Mirror Technologies for Adaptive Optics and Astronomy. *SPIE*, Adaptive Optics Systems III, 2012.

[12] Anne Marinan, Kerri Cahoy, Matthew Webber, Ruslan Belikov, and Eduardo Bendek. Payload characterization for CubeSat demonstration of MEMS deformable mirrors. *SPIE*, 2014.

[13] Anne D. Marinan. *Improving Nanosatellite Capabilities for Atmospheric Sounding and Characterization*. PhD dissertation, Massachusetts Institute of Technology, Department of Aeronautics and Astronautics, June 2016.

[14] James Paul Mason, Matt Baumgart, Bryan Rogler, Chloe Downs, Margaret Williams, Thomas N. Woods, Scott Palo, Phillip C. Chamberlin, Stanley Solomon, Andrew Jones, Xinlin Li, Rick Kohnert, and Amir Caspi. MinXSS-1 CubeSat On-Orbit Pointing and Power Performance: The First Flight of the Blue Canyon Technologies XACT 3-axis Attitude Determination and Control System. *Journal of Small Satellites*, 6(3):651–662, December 2017.

[15] Claire Max. Introduction to Adaptive Optics and its History. *American Astronomical Society 197th Meeting*.

[16] Ryan Melton. Ball Aerospace COSMOS. https://cosmosc2.com/. Accessed in 2020, 2021.

[17] John Merk, Kerri Cahoy, and Ewan Douglas. Deformable Mirror (DeMi) CubeSat System Requirements Review. Technical report, Aurora Flight Sciences, Cambridge, Massachusetts.

[18] Rachel E. Morgan. Optical Modeling and Validation for the Deformable Mirror Demonstration Mission. Master's thesis, Massachusetts Institute of Technology, 2 2020.

[19] Rachel E. Morgan, Ewan S. Douglas, Gregory W. Allan, Paul Bierden, Supriya Chakrabarti, Timothy Cook, Mark Egan, Gabor Furez, Jennifer N. Gubner, Tyler D. Groff, Christian A. Haughwout, Bobby G. Holden, Christopher B. Mendillo, Mireille Ouellet, Paula do Vale Pereira, Abigail J. Stein, Simon Thibault, Xingtao Wu, Yeyuan Xin, and Kerri L. Cahoy. MEMS Deformable Mirrors for Space-Based High-Contrast Imaging. *Micromachines*, 10(6):366, May 2019.

[20] Ben R. Oppenheimer and Sasha Hinkley. High-Contrast Observations in Optical and Infrared Astronomy. *Annual Review of Astronomy and Astrophysics*, 47:253–289, 2009.

[21] Pixelink, a Navitar Company. *Hyperion Camera Line, PL-D775*. https://pixelink.com/products/industrial-cameras/usb-30/125-sensors/pl-d775/.

[22] W. A. Traub and B. R. Oppenheimer. *Exoplanets*, chapter Direct Imaging of Exoplanets, pages 111–156. University of Arizona Press, 2010.

[23] Robert K. Tyson. *Lighter Side of Adaptive Optics*, chapter 4, pages 37–47. SPIE Press Monograph. SPIE, 2009.